

1 Lab 7 (Mobile Phone Sensor Project) Log Book

Sadman Ahmed Shanto

1.1 Table of Contents:

- Background and Theory
- Experiment 1
- Experiment 2
- Project Questions
- Conclusion & Summary

2 Background and Theory:

2.1 Mobile Phone Sensors

As mobile phones have matured as a computing platform and acquired richer functionality, these advancements often have been paired with the introduction of new sensors. For example, accelerometers have become common after being initially introduced to enhance the user interface and use of the camera. They are used to automatically determine the orientation in which the user is holding the phone and use that information to automatically re-orient the display between a landscape and portrait view or correctly orient captured photos during viewing on the phone.

Nowadays, a typical phone houses a suite of sensors that include a gyroscope, compass, accelerometer, proximity sensor, and ambient light sensor, as well as other more conventional devices that can be used to sense such as front and back facing cameras, a microphone, GPS and WiFi, and Bluetooth radios. Many of the newer sensors are added to support the user interface (e.g., the accelerometer) or augment location-based services (e.g., the digital compass).

Applications have been developed that can take advantage of both the low-level sensor data and high-level events, context, and activities inferred from mobile phone sensor data, are being explored not only in academic and industrial research laboratories but also within startup companies and large corporations.

For the purposes of our project, we made use of **triaxial accelerometers** and the following apps for accessing those sensors.

Android App used (02/7/21 -02/13/21): **Physics Toolbox Suite**

Android App used (02/13/21 -02/24/21): **MATLAB**

Apple App used (02/7/21 -02/24/21) : **Phyphox**

The apps have a timing uncertainty of $0.001s$ and accelerometer uncertainty of $0.1ms^{-2}$. [1]



2.2 Triaxial Accelerometer

Triaxial accelerometer is a sensor that returns an estimate of acceleration along the x, y and z axes from which velocity and displacement can also be estimated.

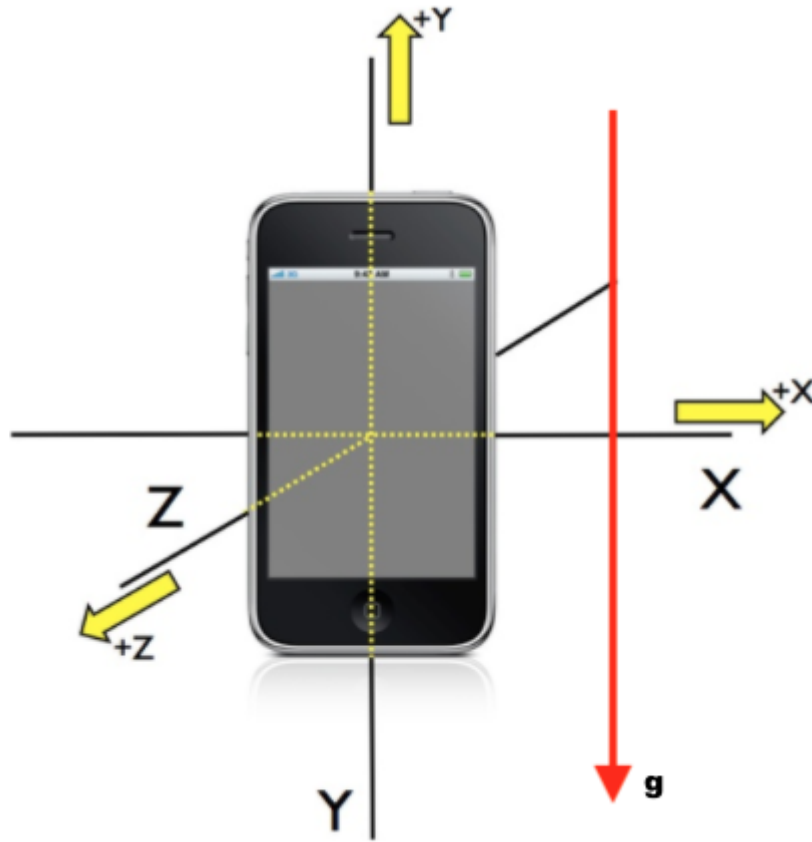


Fig 1: Picture showing the axis of acceleration sensor

These cellphone accelerometer consists of many different parts and works in many ways, two of which are the piezoelectric effect and the capacitance sensor. The piezoelectric effect is the most common form of accelerometer and uses microscopic crystal structures that become stressed due to accelerative forces. These crystals create a voltage from the stress, and the accelerometer interprets the voltage to determine velocity and orientation. The capacitance accelerometer senses changes in capacitance between microstructures located next to the device. If an accelerative force moves one of these structures, the capacitance will change and the accelerometer will translate that capacitance to voltage for interpretation.

2.3 Filters

In signal processing, a filter is a device or process that removes some unwanted components or features from a signal. Filtering is a class of signal processing, the defining feature of filters being the complete or partial suppression of some aspect of the signal through removal of some frequencies or frequency bands.

From elementary literature review on the topic, I understood that there are for common filters.

- **Low-pass filter**, passes signals with a frequency lower than a certain cutoff frequency and attenuates signals with frequencies higher than the cutoff frequency.
- **High-pass filter**, passes signals with a frequency higher than a certain cutoff frequency and attenuates signals with frequencies lower than the cutoff frequency.

- A **band-pass filter** can be formed by cascading a high-pass filter and a low-pass filter.
- A **band-reject filter** is a parallel combination of low-pass and high-pass filters.

For the purposes of our study, we are mostly interested in low-pass filters. The one that we make use of is the **Butterworth Filter**. The frequency response of this filter is maximally flat (i.e. has no ripples) in the passband and rolls off towards zero in the stopband, making it one of the most popular low pass filter.

2.4 Fourier Transform, Discrete Fourier Transform and the Fast Fourier Transform

The Fourier Transform (FT) takes a time-based pattern, measures every possible cycle, and returns the overall "cycle recipe" (the amplitude, offset, & rotation speed for every cycle that was found). In its pure essence, it is an integral transform that maps functions in the temporal space to its associated frequency space.

To apply Fourier Transforms to real world data we need a FT definition for a discrete set of values. This is given by the Discrete Fourier Transform (DFT) which is the FT of a discrete sequence of values. This is derived (informally) by rewriting the function in the FT as a discrete sequence (vector if you like) and replacing the infinite sum, with a sum over a finite number of values. This, however, is a costly operation with a time complexity of $O(N^2)$.

Often cited as one of the most important algorithms of the 20th century, the Fast-Fourier Transform (FFT) is truly what brings the idea of the Fourier Transform into practice. The FFT is an efficient algorithm for computing the DFT. In short, it reduces the computational complexity to $O(N \log(N))$ by using a periodicity in the twiddle factor to avoid calculating the term that gives you the same value as the one you already calculated before and avoid calculating the same term across DFT components so that you could simply recall the value that you used before.

2.5 Experiments Chosen:

1. Extraction of the value of g from accelerometer data
2. Fourier Analysis of Human Motion Data

3 Experiment 1: *Extraction of the value of g from accelerometer data*

3.1 Methodology

- We have time series acceleration data in three dimensions - x , y , z .
- Each time series \rightarrow linear acceleration of body + linear acceleration due to gravity
- We use a digital low pass filter in order to separate the AC component from the DC component in each time series.
 - AC component (high frequency) \rightarrow dynamic motion of body
 - DC component (low frequency) \rightarrow influence of gravity

- Set Cut-Off frequency, record sampling rate and solve for the coefficients - a and b - where A_{DC} is filtered output data and A is raw input data.

$$A_{DC}[n] = aA[n] + bA_{DC}[n - 1]$$

- Repeat the process for all spatial axes and store the low pass filter time series
- Calculate the magnitude of the low pass filter time series.

$$A_g = \sqrt{(A_{DC_x}^2 + A_{DC_y}^2 + A_{DC_z}^2)}$$

- g is the arithmetic mean of the low pass filter time series, A_g

$$g = \text{mean}(A_g)$$

3.2 Data From Mohammad's Drive From LBK to DFW

Mohammad recorded a data set while driving from Lubbock to Dallas. We are using this dataset to try and extract the gravitational field strength, g , information from. If time permits, we also plan on performing some other experiments using this data set.

The data set contains information for roughly 2.68 hours.

Out[1]:

	time	gFx	gFy	gFz	ax	ay	az	wx	wy	wz	...	Bx
1	0.056	0.1107	0.5201	1.0128	0.0000	0.0000	0.0000	0.0000	0.0000	0.0000	...	0.0000
2	0.056	0.1107	0.5201	1.0128	0.0000	0.0000	0.0000	0.0000	0.0000	0.0000	...	0.0000
3	0.068	0.1142	0.4607	0.9509	0.0000	0.0000	0.0000	0.0000	0.0000	0.0000	...	0.0000
4	0.085	0.0506	0.4603	0.8793	0.0000	0.0000	0.0000	0.0000	0.0000	0.0000	...	0.0000
5	0.085	0.0506	0.4603	0.8793	0.1625	0.1021	0.2422	0.0000	0.0000	0.0000	...	0.0000
...
469700	9637.865	0.0426	0.4406	0.9823	-0.6587	0.0841	-0.0047	-0.2531	-0.0021	0.0393	...	7.722
469701	9637.879	0.0928	0.4476	1.0419	-0.6587	0.0841	-0.0047	-0.2531	-0.0021	0.0393	...	7.722
469702	9637.880	0.0928	0.4476	1.0419	-0.1249	0.0939	0.8053	-0.2531	-0.0021	0.0393	...	7.722
469703	9637.888	0.0600	0.4377	1.0173	-0.1249	0.0939	0.8053	-0.2531	-0.0021	0.0393	...	7.722
469704	9637.889	0.0600	0.4377	1.0173	0.4114	0.1872	1.3678	-0.2531	-0.0021	0.0393	...	7.722

469704 rows × 21 columns

The collected data set contained the above information. Note that we are also provided with the gForce data which we might use later for verification of our analysis. Now, lets make the acceleration plots.

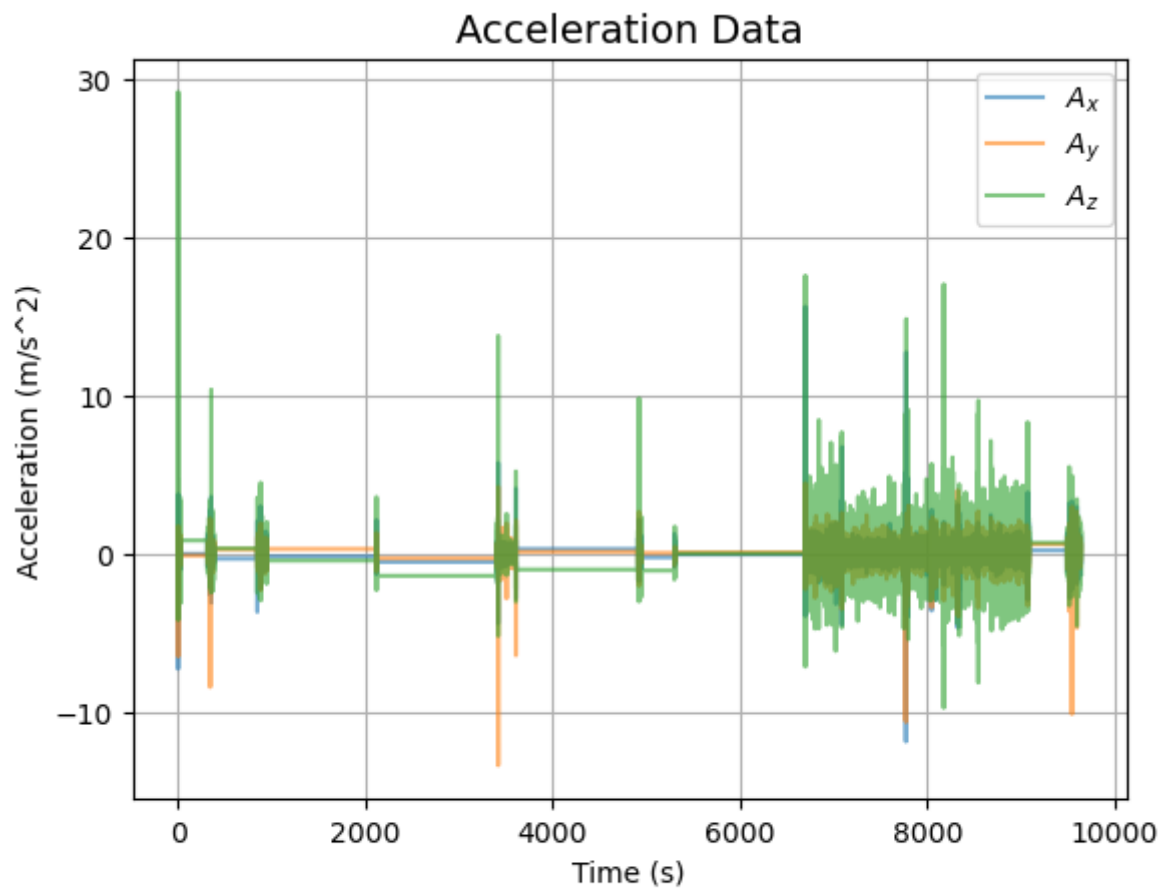


Fig 2: Acceleration Data in x, y, z direction

Fig. 2 shows how Mohammad's car acceleration vector was changing throughout his journey.

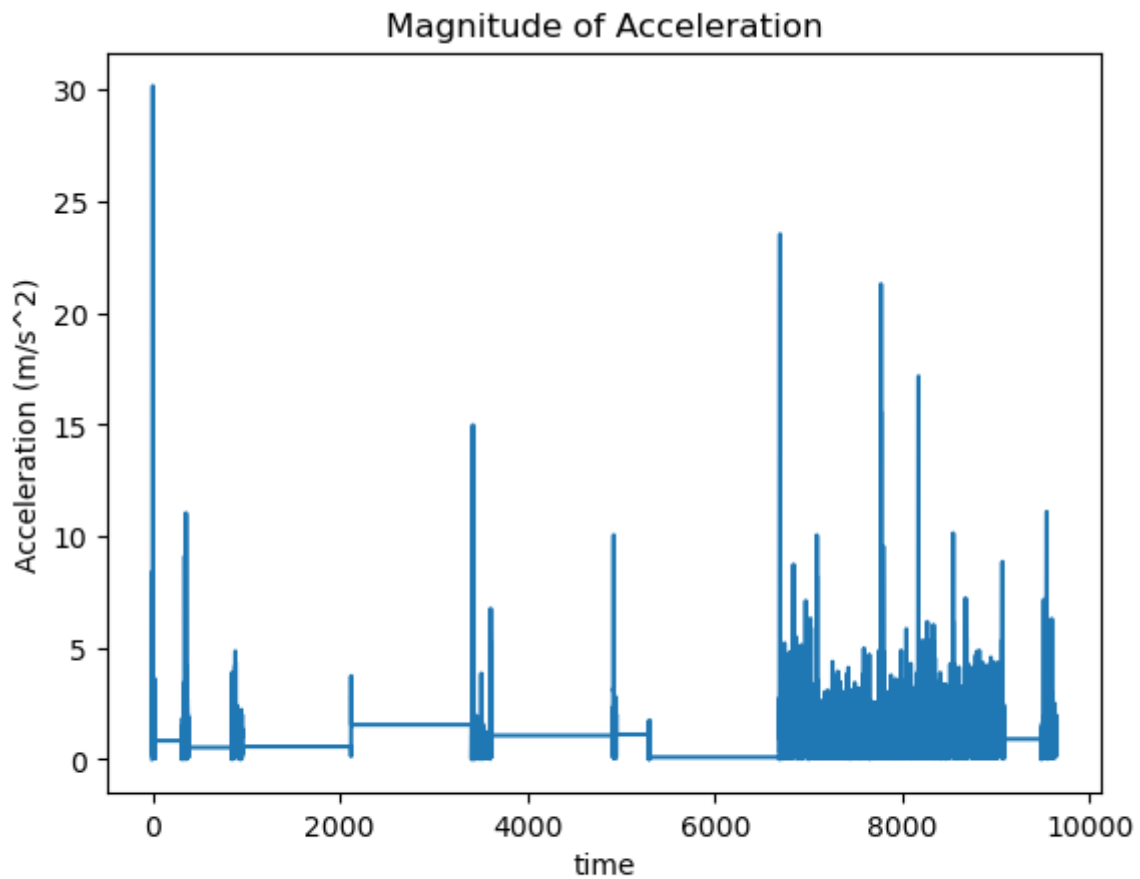


Fig 3: Magnitude of Acceleration

Fig. 3 shows how the absolute acceleration of his Car is changing over time. Now that we have such data. We need to implement the filters to extract the value of g .

Applying the low pass filter to the accelerometer dataset. As mentioned in **Section 2.3**, we

implement the Butter Low Pass filter of order 4, sample rate, $f_{sr} = 10Hz$ (obtained from the App) and cutoff_frequency, $f_{co} = 0.1Hz$ [2].

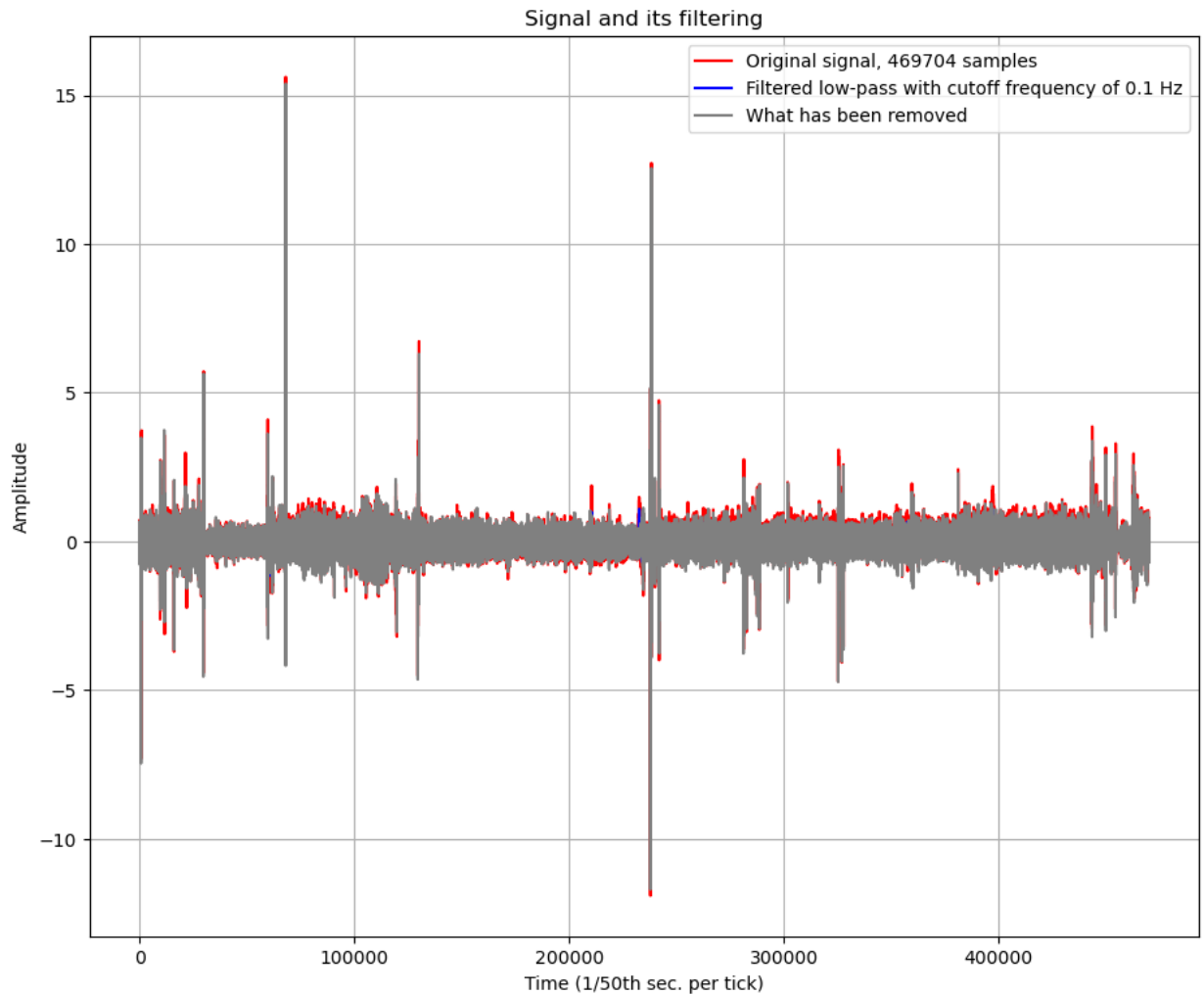


Fig 4: Signal Analysis of A_x

Fig. 4 shows the original Acceleration data in x-axis (red), the low pass filtered output acceleration data (due to gravity) (blue). It also shows how our filter has works. Now that we have this data, we calculate the value of g from the filtered data set.

Out[31]: 0.19378453626170816

The value of calculated g is $\sim 0.19 \frac{m}{s^2}$ which is in no where close to the expected value of $9.81 \frac{m}{s^2}$. The difference points out either our data acquisition or the filtering process is incorrect.



3.3 Data From Mohammad's Flight From IAH to LBK

Mohammad recorded a data set while flying from Houston to Lubbock. We are using this dataset to try and extract the gravitational field strength, g , information from. We are using the same device (Mohammad's phone) and same app to investigate what caused the error from the previous run.

Out[10]:

	time	gFx	gFy	gFz	ax	ay	az	wx	wy	wz	...
1	0.183	-0.0262	0.7371	0.6736	0.0000	0.0000	0.0000	0.0000	0.0000	0.0000	...
2	0.213	-0.0262	0.7371	0.6736	0.0000	0.0000	0.0000	-0.0326	-0.0304	0.0131	...
3	0.224	-0.0262	0.7371	0.6736	0.0000	0.0000	0.0000	-0.0326	-0.0304	0.0131	... -1
4	0.244	-0.0262	0.7371	0.6736	0.0000	0.0000	0.0000	-0.0326	-0.0304	0.0131	... -1
5	0.245	-0.0262	0.7371	0.6736	0.0000	0.0000	0.0000	-0.0326	-0.0304	0.0131	... -1
...
137487	13492.824	-0.0131	0.1868	0.9797	-0.0132	-0.0132	-0.0035	-0.0001	-0.0013	0.0005	... -1
137488	13492.835	-0.0131	0.1868	0.9797	-0.0132	-0.0132	-0.0035	0.0822	-0.0195	0.0001	... -1
137489	13492.844	-0.0131	0.1868	0.9797	-0.0198	-0.0491	0.0288	0.0822	-0.0195	0.0001	... -1
137490	13492.845	-0.0131	0.1868	0.9797	-0.0198	-0.0491	0.0288	0.0822	-0.0195	0.0001	... -1
137491	13492.866	-0.0105	0.1954	0.9476	-0.0198	-0.0491	0.0288	0.0822	-0.0195	0.0001	... -1

137491 rows × 21 columns

The accelerometer plots are as follows:

Ax, Ay, Az Plots

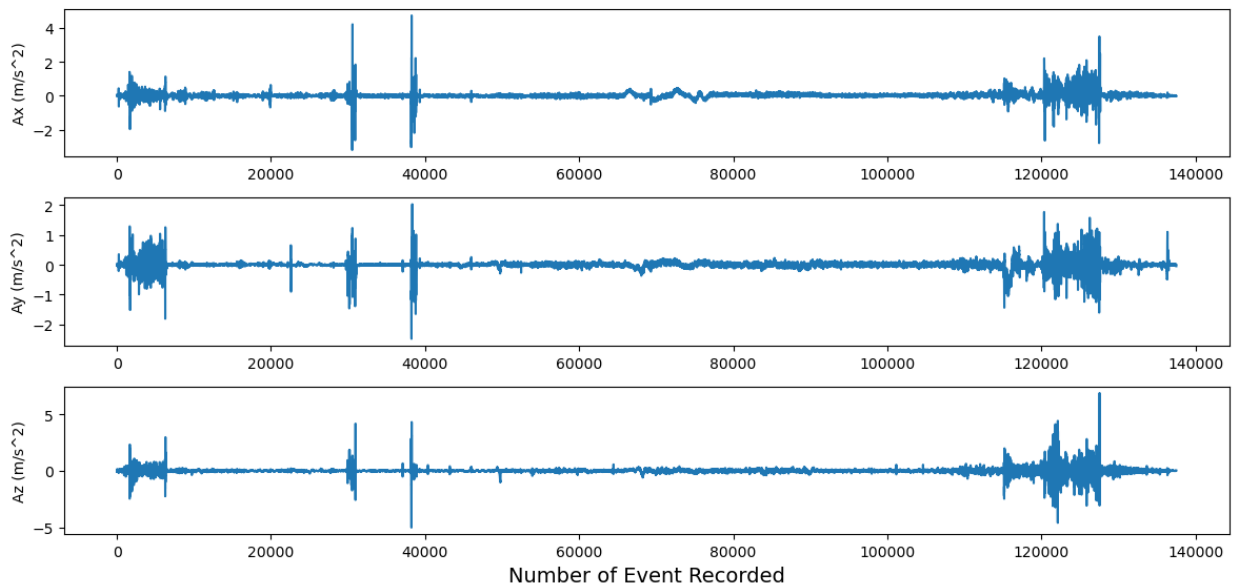


Fig 5: Acceleration Data in x, y, z direction from Flight Data Set

Fig. 5 shows how the acceleration of Mohammad's flight was changing. Looking at the filtered acceleration data after implementing the Low Pass Filter.

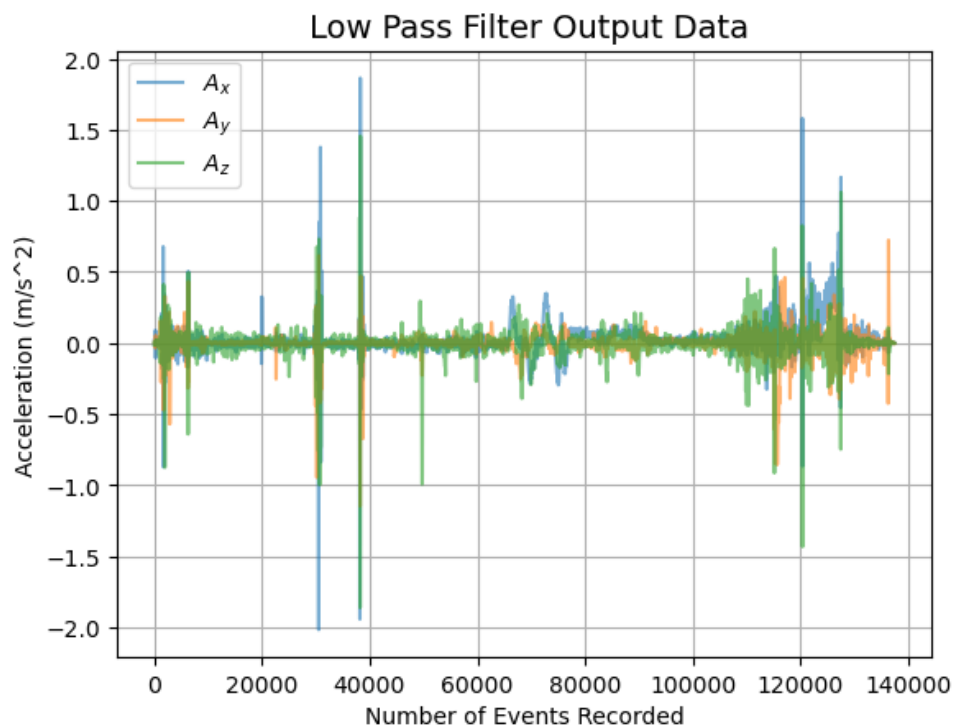


Fig 7: Plot of Low Pass Filter Output Data for Acceleration in x, y, z direction

Fig. 7 shows the low pass filter output acceleration data in the three dimensions. Using this data set to estimate the value of g (ms^{-2}).

```
Out[51]: 0.10478987781472546
```

Again, we miscalculate the value of g . As a sanity check we use the GForce Data Sensor to estimate the value of g (ms^{-2}).

GForce Plots

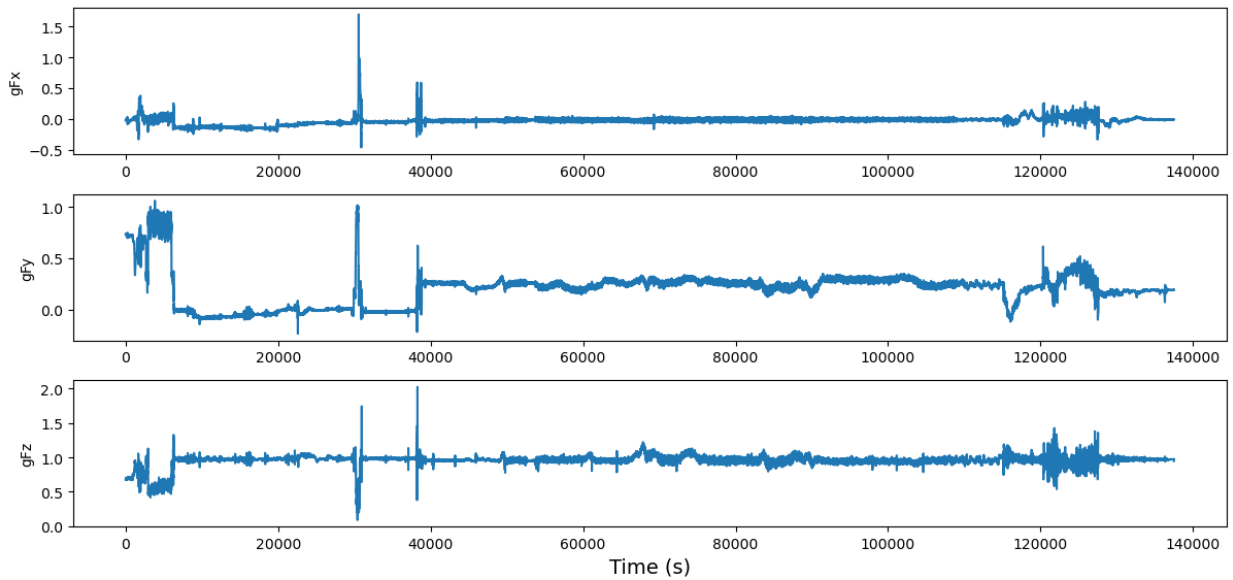


Fig 8: Plot of GForce x, y, z direction

Fig. 8 is a plot of how the GForce was changing through out the flight. The GForce in this context is defined such that $\text{GForce} = 1$ means 9.81 m/s^2 . Taking the average of the euclidean norm of the GForce data in the x , y , z direction and multiplying by 9.81 we can calculate the value of g from this dataset. We find it to be as follows:

Out[54]: 9.765305419677741

As evident, the sensor is clearly detecting the gravitational acceleration ($g \sim 9.77 \text{ m/s}^2$). We are now looking more into the app to see how it functions.

At the 11th hour, we realized that the app we have been using **already filters the accelerometer data** by isolating the effects of gravity - the same task we wanted to undertake. Now, we have decided to move to a different app to record the raw acceleration data since there was no options

to stop the app from filtering the data.

We are choosing **MATLAB**'s mobile app to work as the sensor since it does not autofilter.



3.4 10 Hour Data Set From Mohammad's Home Activities

We have recorded a 10 hour data run using the new app. Mohammad acquired all this data while doing his every day activities at home. The following is how the data looks like.

Out[16]:

	timestamp	X	Y	Z
0	0.000	0.216850	0.030808	9.649057
1	0.100	0.230608	0.029910	9.652946
2	0.200	0.237488	0.010469	9.652946
3	0.300	0.215354	0.019442	9.649955
4	0.400	0.204586	0.019143	9.648160
...
298402	36090.907	0.089133	0.173779	9.682557
298403	36091.007	0.083749	0.171685	9.685847
298404	36091.107	0.080459	0.177667	9.682557
298405	36091.207	0.085843	0.171685	9.685847
298406	36091.307	0.083450	0.179462	9.681062

298407 rows × 4 columns

The accelerometer plot is as follows

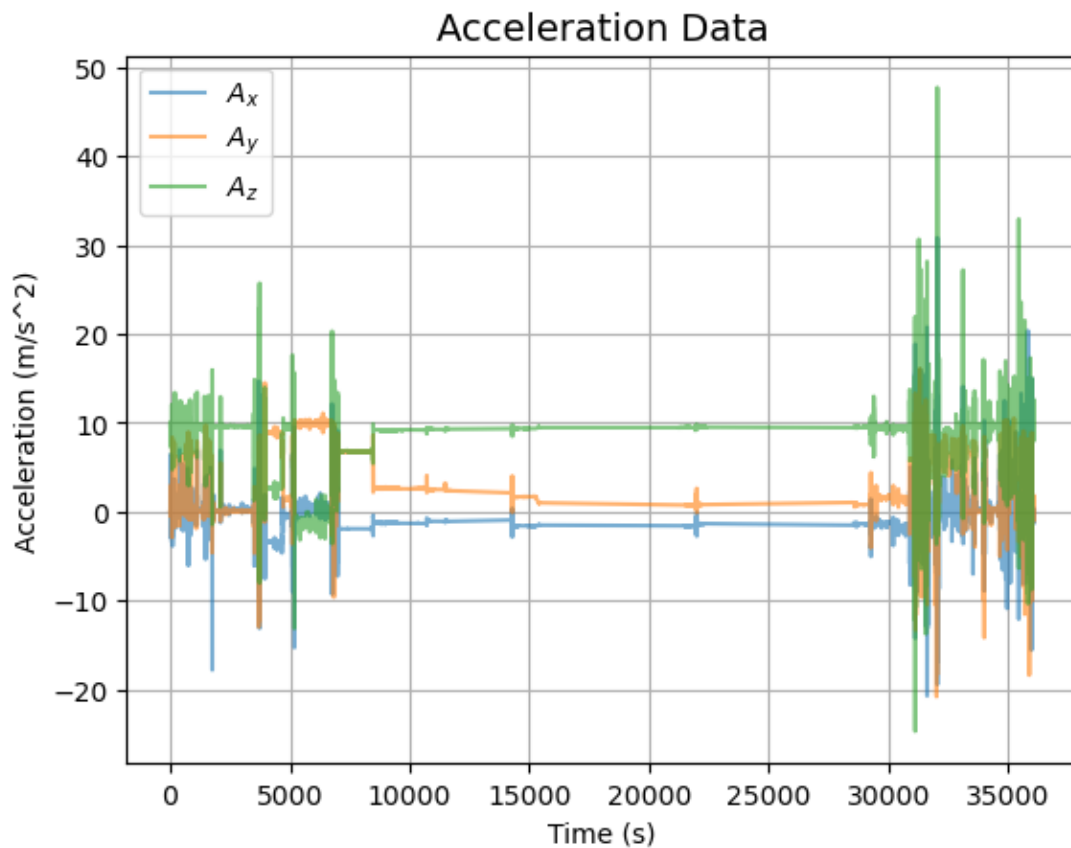


Fig 9: Acceleration in x, y, z direction for Mohammad Home Data

Fig. 9 shows how the accelerator data from Mohammad's phone. The fluctuations in this plot reflect Mohammad's activities while the period of linear relation is when he was sleeping. Now, trying to calculate the g value from this data set using the same routine as before.

Out[126]: 9.711021311356017

Calculating the error in our calculated value using

$$error = \frac{|g_{calc} - g_{real}|}{g_{real}} * 100$$

Out[127]: 1.0192407726285004

Beautiful! As we can see our filtering algorithm is almost near spot on (within 1% error). This is really promising since Mohammad did not keep his device oriented in a particular axis throughout the duration of the experiment which introduces inconsistencies in the Acceleration data. However, taking the Euclidean Norm in 3 dimensions may have mitigated the error's impact on our final result.

We can try and calibrate this data even further by filtering out the effects of Mohammad rotating his phone. For this, we can use the gyroscope in his device.

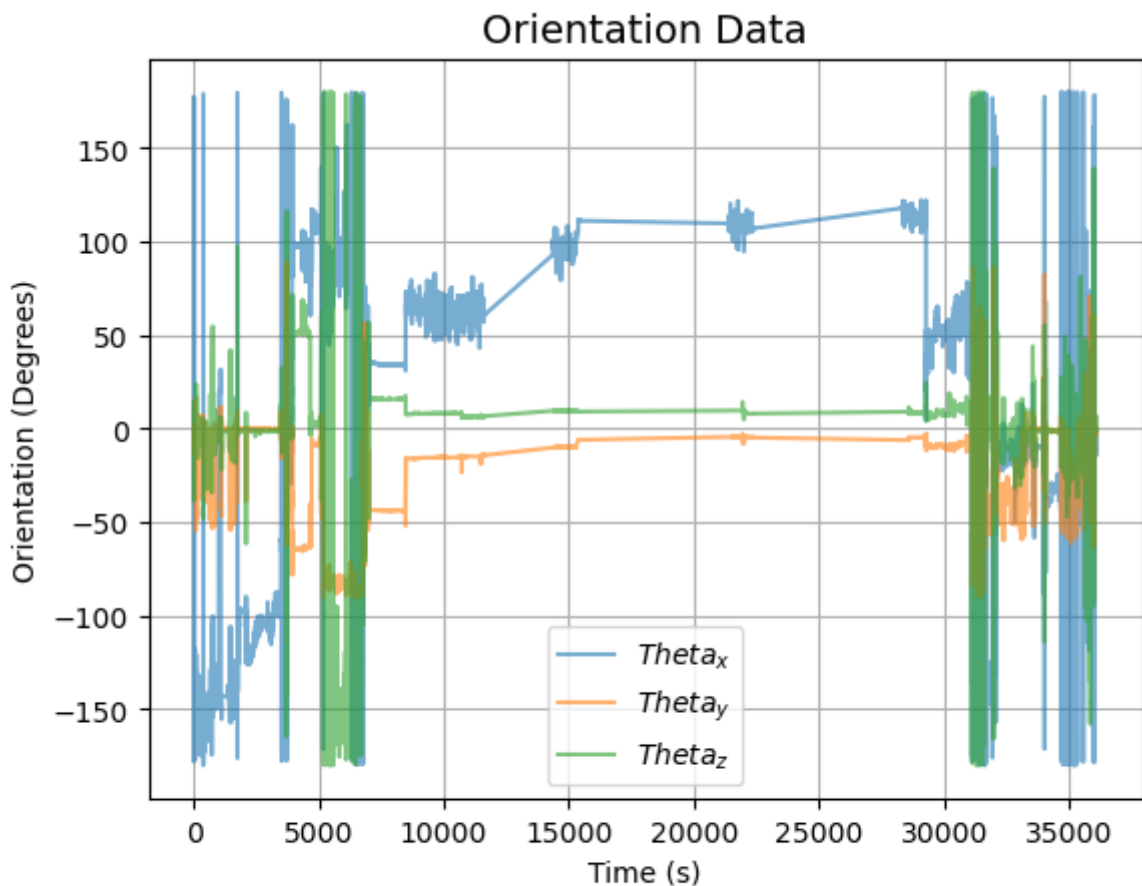


Fig 10: Mohammad's Phone Orientation Data

Fig. 10 shows how Mohammad's phone was oriented with respect to a fixed axis system. It clearly shows how he was using his phone (time period 0 to 5000s and 30000 to 35000) while he was sleeping the orientation was more or less constant. The fluctuations while he was sleeping was due to the fact that he had he his phone on his bed and Mohammad confessed to be a "tossy-turner" sleeper. Creating a histogram with this orientation data.

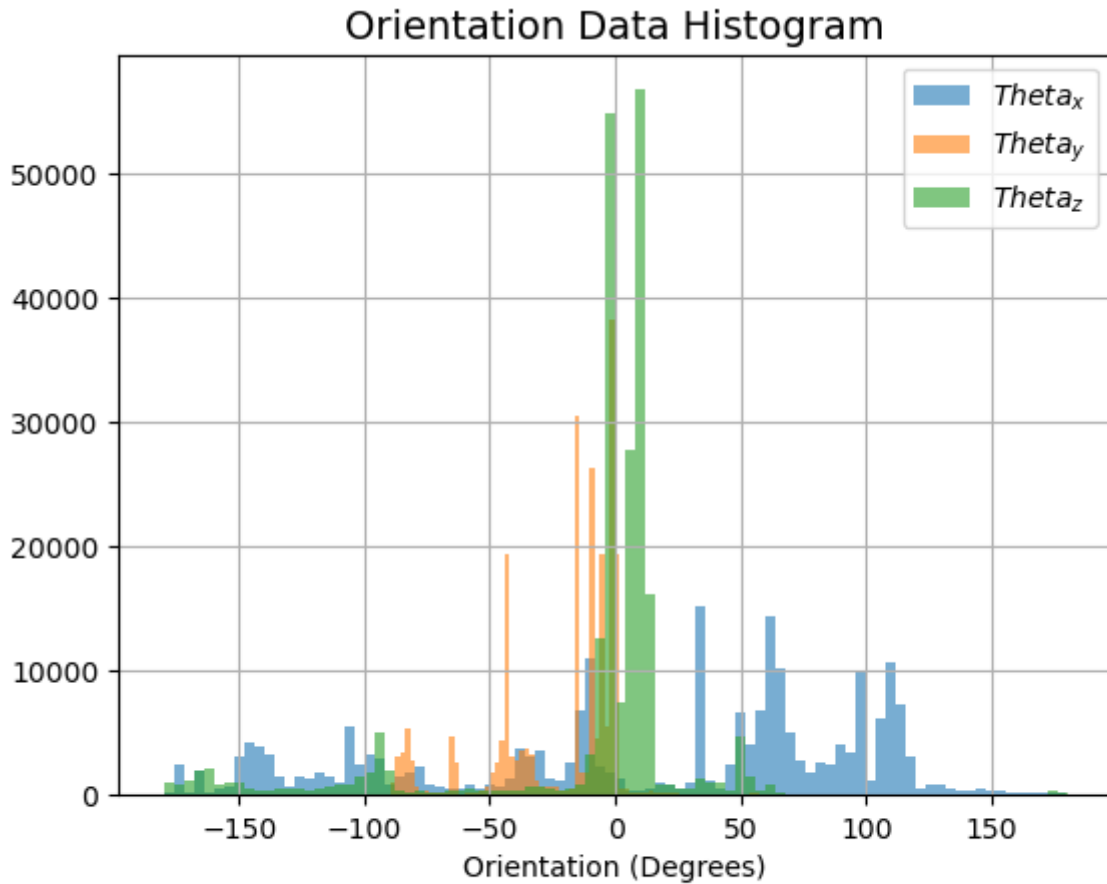


Fig 11: Histogram of Mohammad's Phone Orientation Data

The histogram shows how often Mohammad kept his phone stationary while using and how often he was using it in some orientation that is not the static axes. Keeping events that are within ± 5 degrees orientation to 0 degrees to minimize the effects of changing orientation effects. Using this trimmed dataset, we get the following value for $g(m_s^{-2})$

Out[142]: 9.793524211722861

Calculating the error (%) of the difference between the recorded data and accepted data for g .

Out[141]: 0.16823145499980302

As expected the calibration helped reduce the overall error from 1.02% to 0.168% an improvement factor of almost 600%.

4 Experiment 2: Fourier Analysis of Human

Motion Data

The purpose of this experiment is to analyze the time series acceleration data that Mohammad and Sam generates (while doing certain activities) in Fourier Space. The goal of this study is to answer the following questions:

- Can we identify distinct activity signatures from acceleration data in Fourier Space?
- Are there activity dependent frequencies that are universal?

4.1 Methodology

Mohammad and Sam were to record data while keeping the phones in a fixed orientation attached to their body (Phone was held upright at center of chest with phone screen facing towards body). The y direction is the direction parallel to gravitational acceleration, z direction is perpendicular to the chest pointing outwards, and x being parallel to the shoulders. After the data is generated, we take Fourier Transforms of the acceleration data and analyze the power spectrum to try and answer the research questions we defined earlier.

4.2 Data Set 1: 1 Hour Activity From Sam

Sam took data for an hour while he was working on some homework, walked around and then drove to work.

Out[25]:

	time	ax	ay	az
0	0.000000	-0.079784	9.879006	-0.205972
1	0.100796	-0.066911	9.868379	-0.197888
2	0.201627	-0.063318	9.870923	-0.185913
3	0.302457	-0.071851	9.867331	-0.181423
4	0.403287	-0.068557	9.873019	-0.189805
...
71312	7174.506640	-0.713267	9.544003	1.810784
71313	7174.605486	-1.122665	9.800869	1.688489
71314	7174.704333	-0.678090	9.676927	1.494941
71315	7174.803179	-0.998124	9.653126	1.634601
71316	7174.902025	-0.983904	9.431138	2.084116

71317 rows × 4 columns

The following is the plot for the acceleration data.

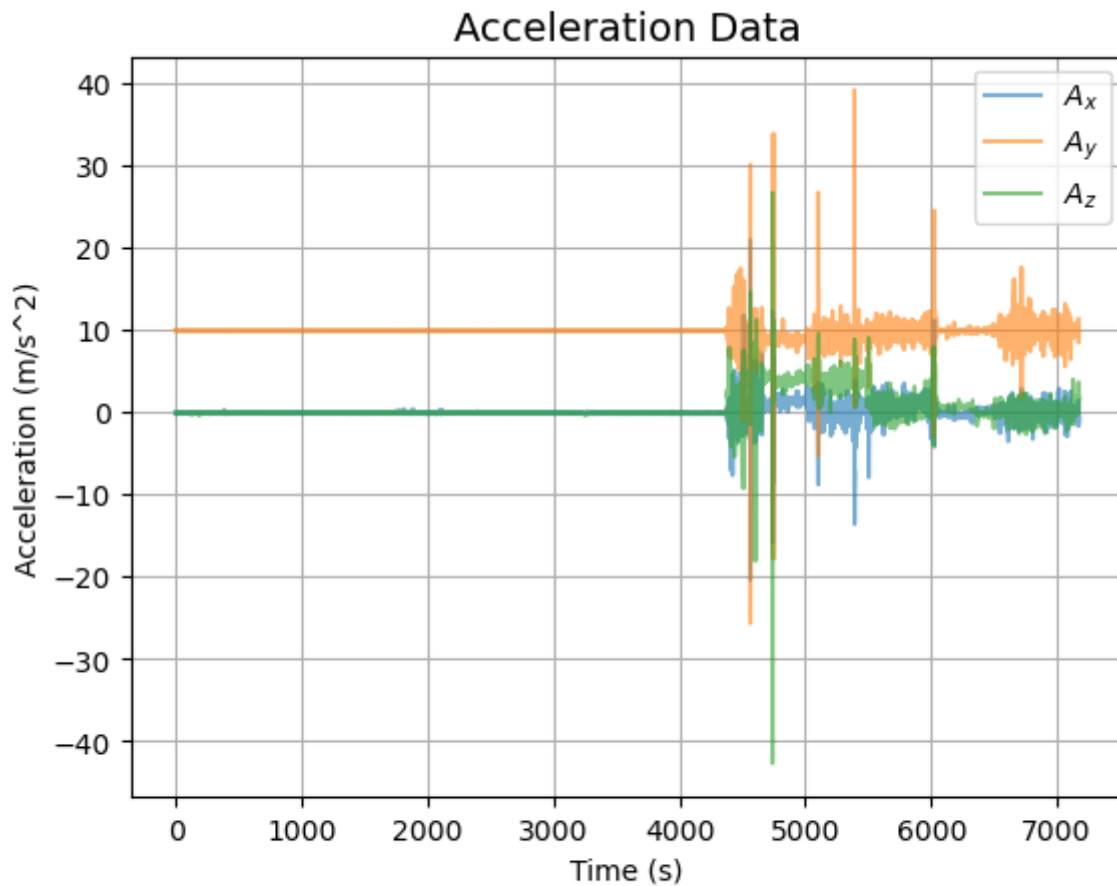


Fig 12: Acceleration Data in x, y, z direction from Sam

Fig. 7 shows how the acceleration data in the three dimensions changed while Sam was taking data. As seen, Sam was not using his phone for the first 4500 seconds as he was doing homework. The other part shows the acceleration as Sam walked from his house to car and then drove to work.

Taking the Fourier Transform of this dataset we create the following power spectra plots.

Fourier transform depicting the frequency components (Sam)

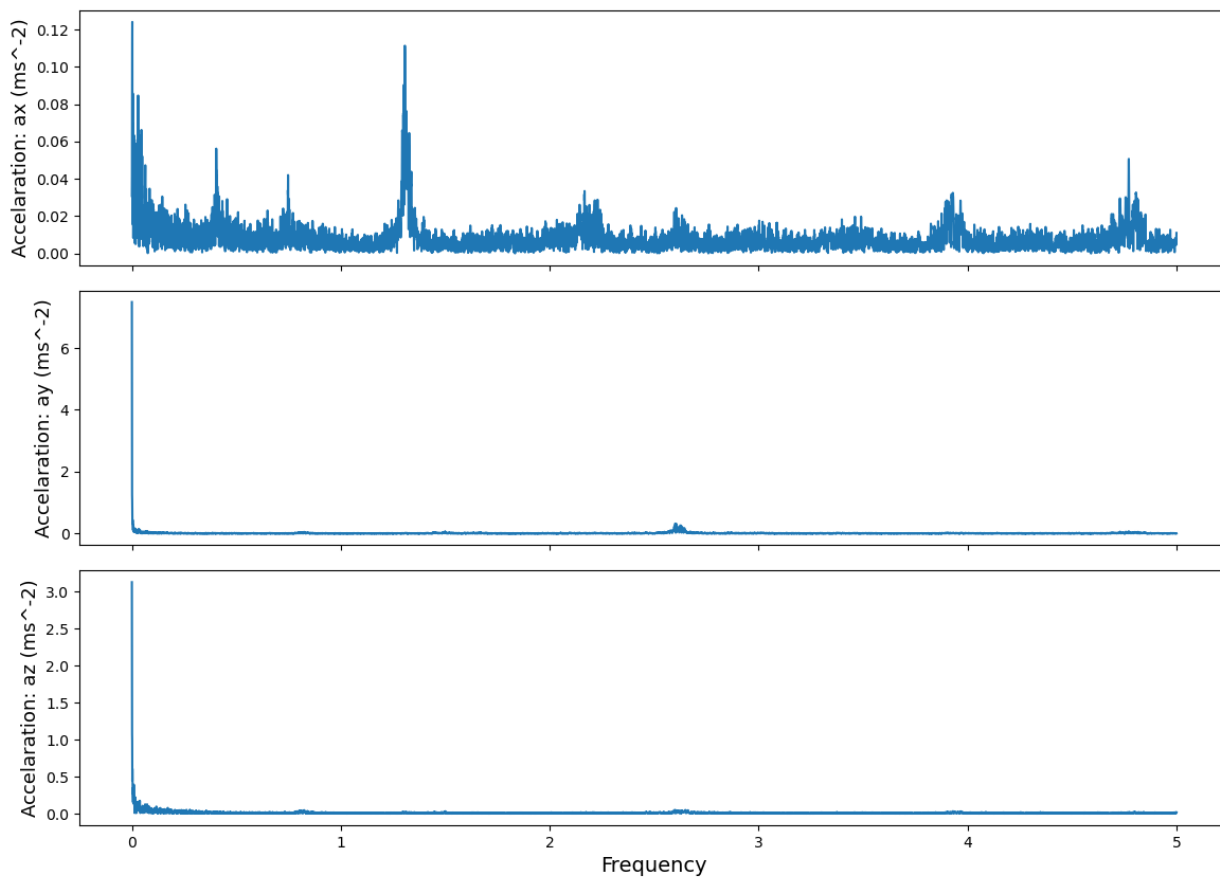


Fig 13: Fourier Transform of Accelerometer Data in x, y, z direction

The power spectra clearly shows the influence of gravity in the lower frequency end (the tall peak around 0) in all directions. We can also observe smaller amplitude higher frequency signals that are more characteristic of Sam's motions.



4.3 Data Set 2: 5 Mins Activity From Mohammad

Mohammad took some data while going down the elevator and walking to his apartment office to pick up a package and later walked three flights of stairs up.

Out[28]:

	time	ax	ay	az
0	0.000	0.190828	9.652946	2.177469
1	0.100	0.364905	9.633504	2.354238
2	0.200	0.637687	9.564411	2.561816
3	0.300	0.597907	9.772287	2.530410
4	0.400	0.703191	9.596416	2.541477
...
3028	261.897	-0.030808	2.179562	9.658031
3029	261.997	0.348455	2.508875	9.102596
3030	262.097	0.249452	2.540280	9.650852
3031	262.197	0.312562	2.656631	9.282657
3032	262.297	0.168395	2.781357	9.018847

3033 rows × 4 columns

The following is how his acceleration varied during the period of data taking.

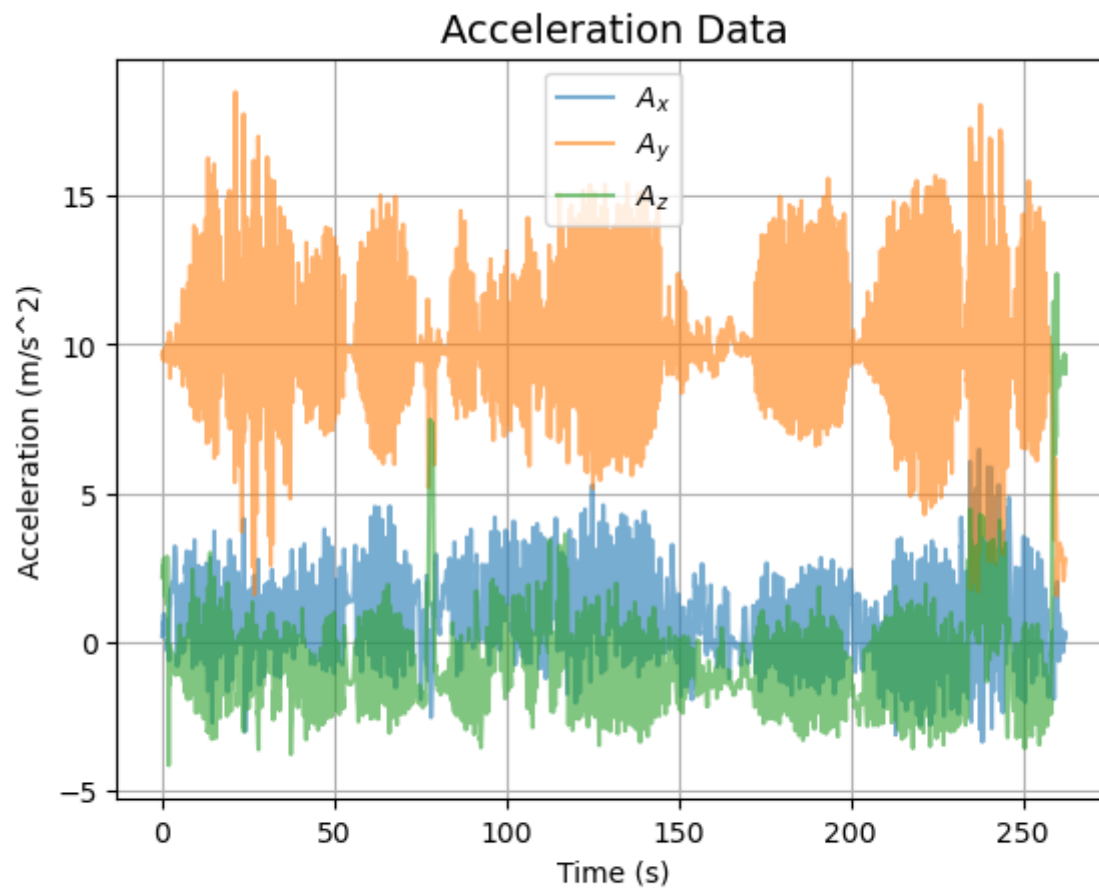


Fig 14: Acceleration Data in x, y, z direction from Mohammad

Fig. 14 Shows Mohammad's acceleration was changing throughout the data taking period. Applying Fourier Transform to this dataset and looking at the power spectrum.

Fourier transform depicting the frequency components (Mohammad)

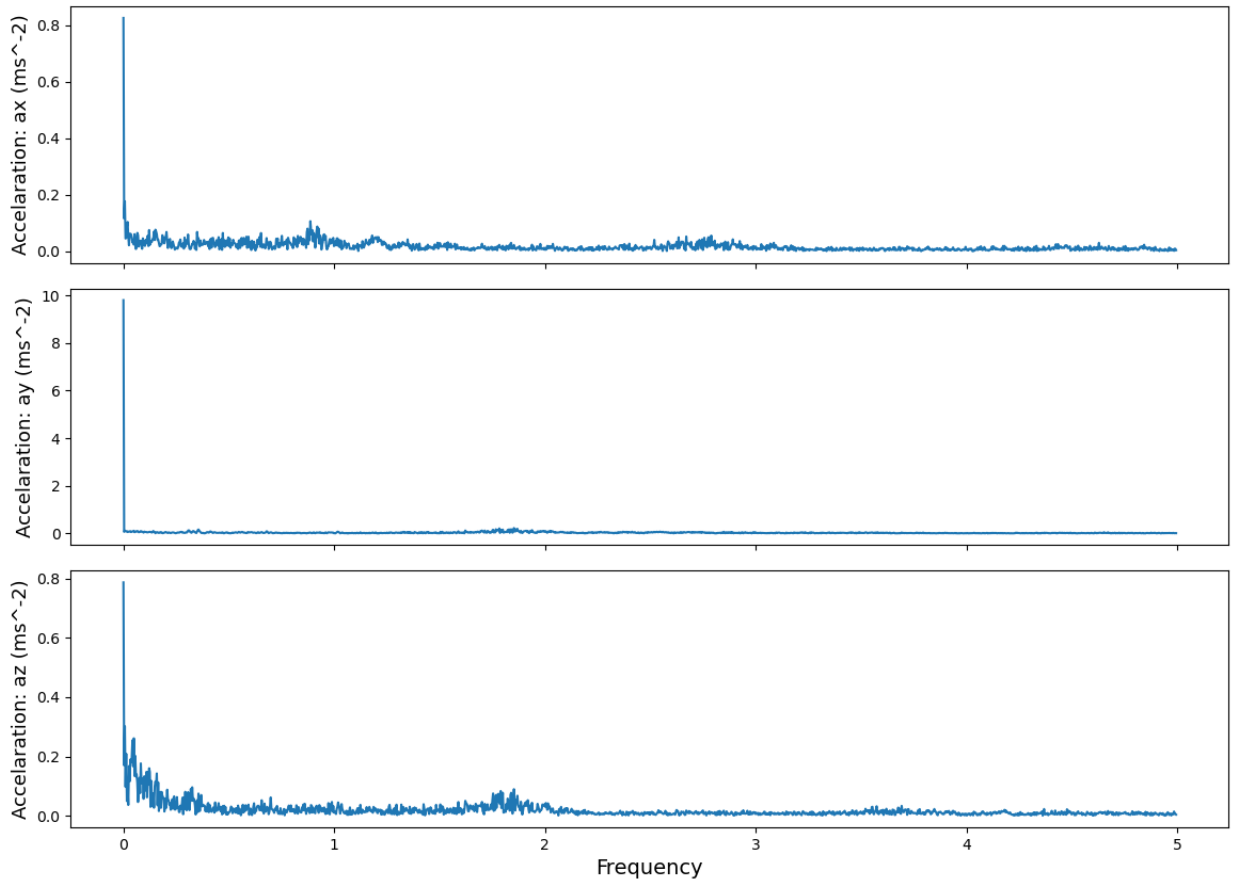


Fig 15: Fourier Transform of Accelerometer Data in x, y, z direction

These plots also show the influence of gravity in the lower frequency end (the tall peak around 0) in all directions similar to Sam's. Unlike Sam's, we observe more prominent smaller amplitude higher frequency signals that reflect Mohammad's activities.

These two data sets were quite rough due to poor experimental design on our part since the choice of activities and their decisions were not made a-priori. This lead to the two data sets - one from Sam and one from Mohammad - to be of different sizes (1 hour and 5 minutes respectively) and had different activities under consideration.

Thus, we planned on taking another data run where Mohammad and Sam would be doing similar activities (5 minutes each) - *walking, jogging/running, chores, sitting, and laying*.



4.4 Data Set 3: Ordered Activity Data From Sam

Sam recored data in the following order in 5 minute blocks.

- jogging (2.46m/s)
- walking
- stairmaster(45 spm)
- chores
- sitting
- lay

Out [32] :

	time	ax	ay	az	activity
0	0.000000	-4.558770	13.991255	10.623259	jog
1	0.100952	-2.477199	12.424763	5.951324	jog
2	0.201873	0.396675	5.089117	3.673960	jog
3	0.302825	0.997975	2.584076	2.921026	jog
4	0.403747	-0.380359	18.807041	14.124328	jog
...
19459	1961.061473	-0.077389	-0.029788	9.814191	lay
19460	1961.162395	-0.059576	-0.024848	9.806258	lay
19461	1961.263286	-0.073647	-0.028441	9.772278	lay
19462	1961.364208	-0.086819	-0.016466	9.802216	lay
19463	1961.465129	-0.072000	-0.029040	9.803563	lay

19464 rows × 5 columns

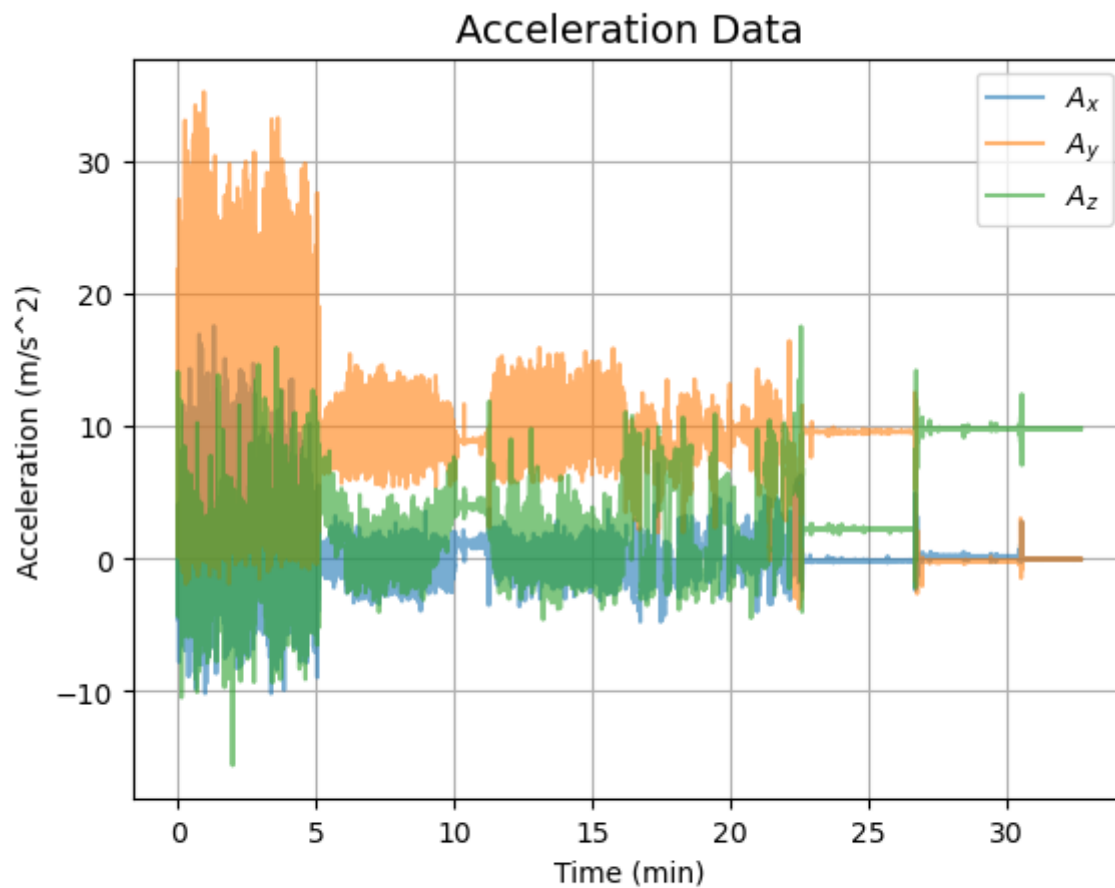


Fig 16: Acceleration Data in x, y, z direction from Sam

Just by eyeballing the plot (Fig. 16) it is clear that the accelerometer data reflects the different classes of activities that Sam undertook. Now looking at the Fourier transform.

Fourier transform depicting the frequency components (Sam)

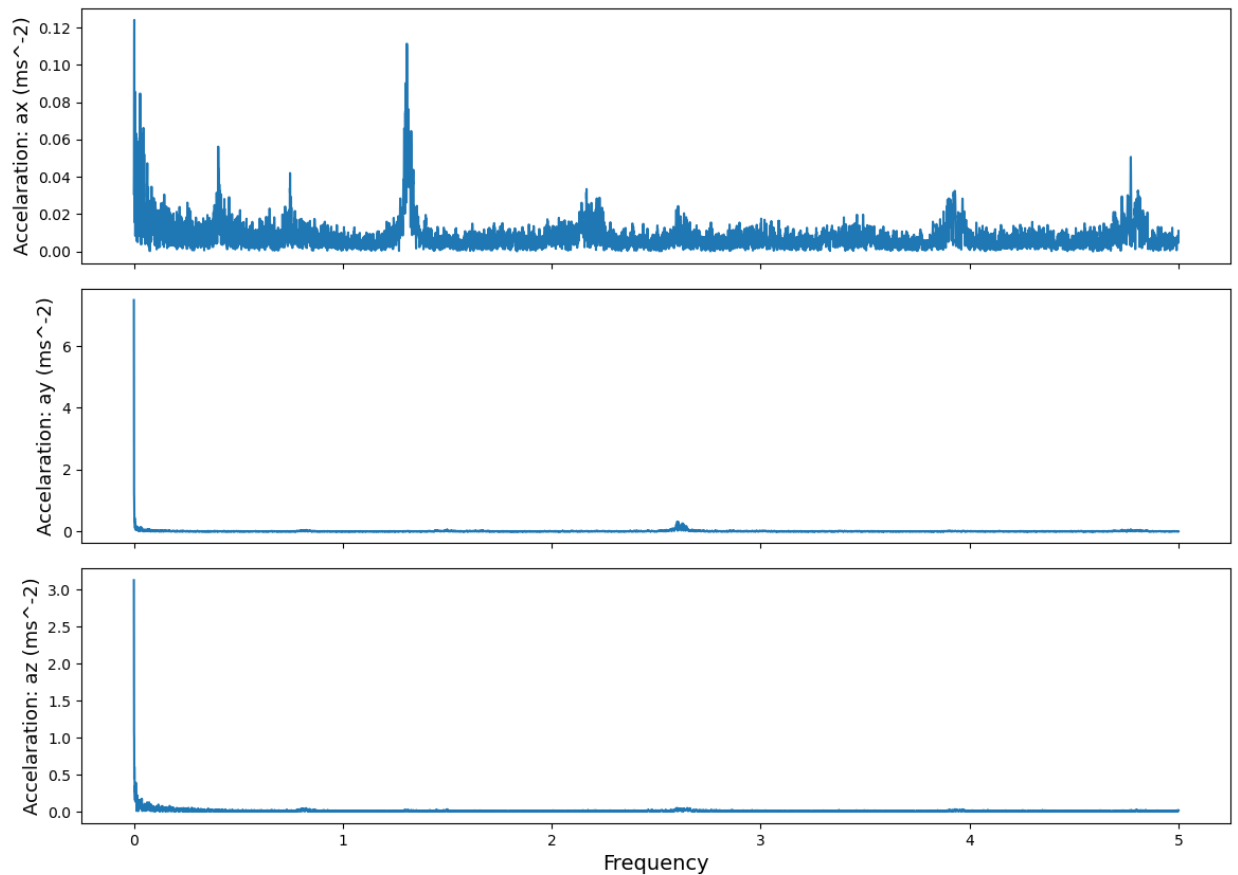


Fig 17: Fourier Transform of Accelerometer Data in x, y, z direction

Fig. 17 is not very informing since the signal representing g is the most prominent. Thus, we need to filter the gravitational data and use a dataset that is representative of only Sam's motions.

Out[36]:

	time	ax	ay	az	activity
0	0.000000	-0.560618	0.944762	-0.897444	jog
1	0.100952	1.412253	-0.529077	-5.084101	jog
2	0.201873	4.176222	-7.770004	-6.879832	jog
3	0.302825	4.666611	-10.178475	-7.155530	jog
4	0.403747	3.176563	6.142691	4.519876	jog
...
19459	1961.061473	-0.004785	-0.008632	0.018720	lay
19460	1961.162395	0.013029	-0.003691	0.010783	lay
19461	1961.263286	-0.001041	-0.007283	-0.023199	lay
19462	1961.364208	-0.014212	0.004693	0.006736	lay
19463	1961.465129	0.000607	-0.007880	0.008081	lay

19464 rows × 5 columns

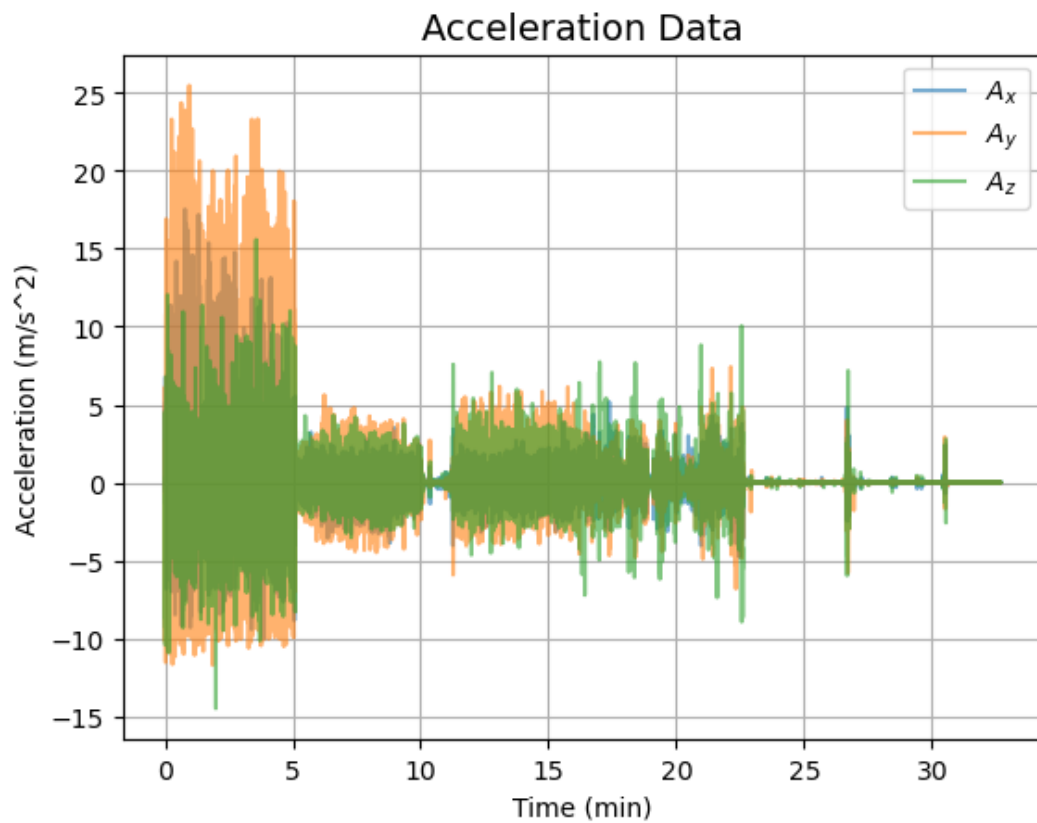


Fig 18: Acceleration Data in x, y, z direction from Sam (No Gravity)

Fig. 18 is the accelerometer with the influence of gravity filtered away.

Fourier transform depicting the frequency components (Sam)

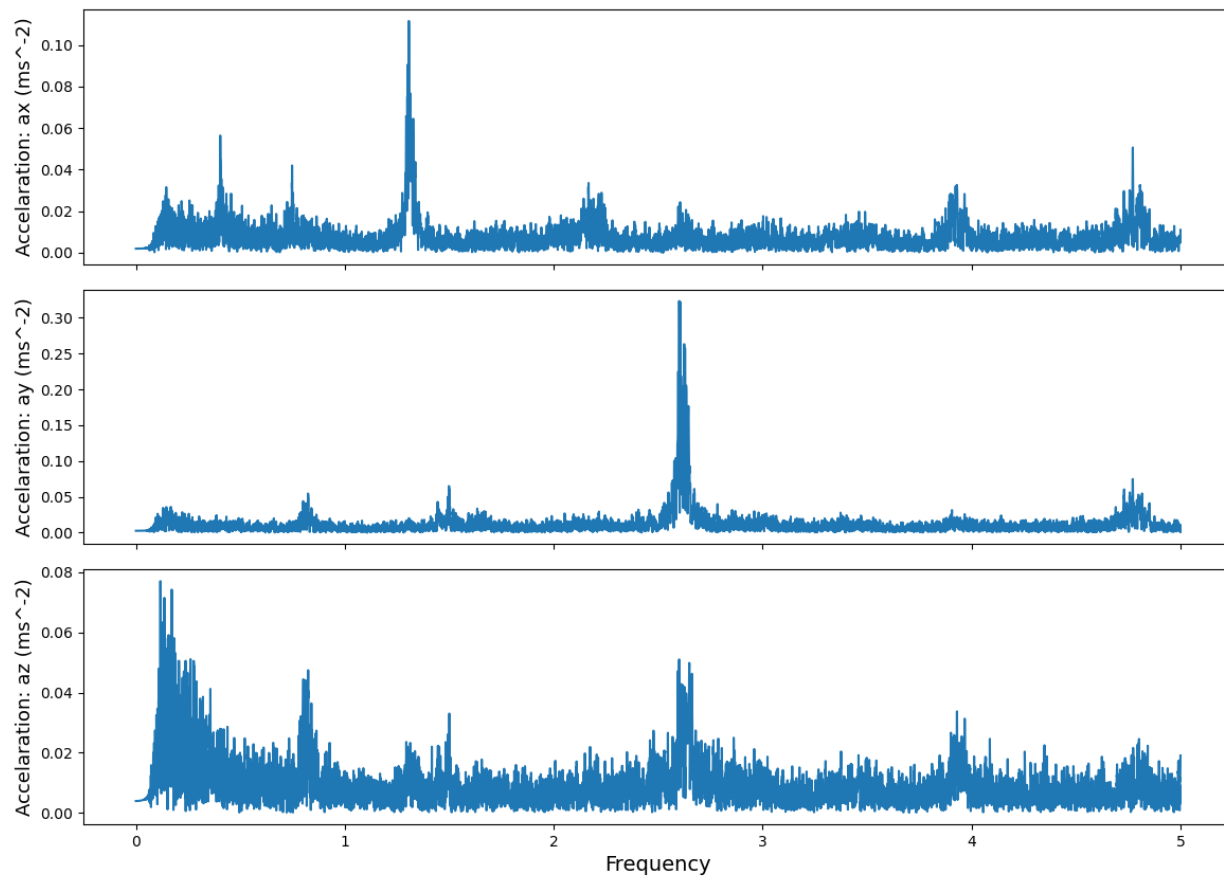


Fig 19: Fourier Transform of Accelerometer Data in x, y, z direction

Fig. 19 shows clearly that there are prominent trends in the power spectrum. To understand what activity is responsible for what we need to isolate them and color code them.

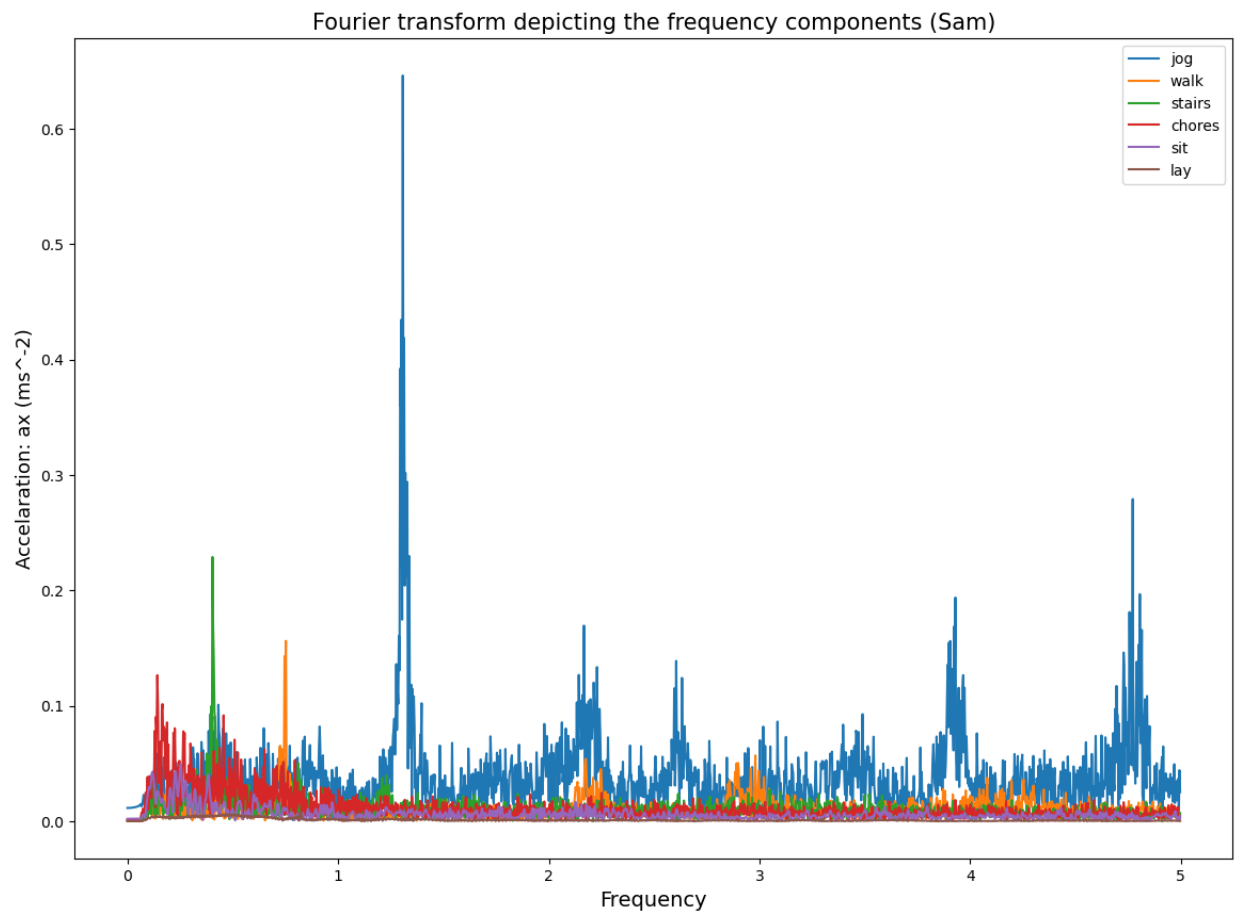


Fig 20: Fourier Transform of Accelerometer Data in ax direction

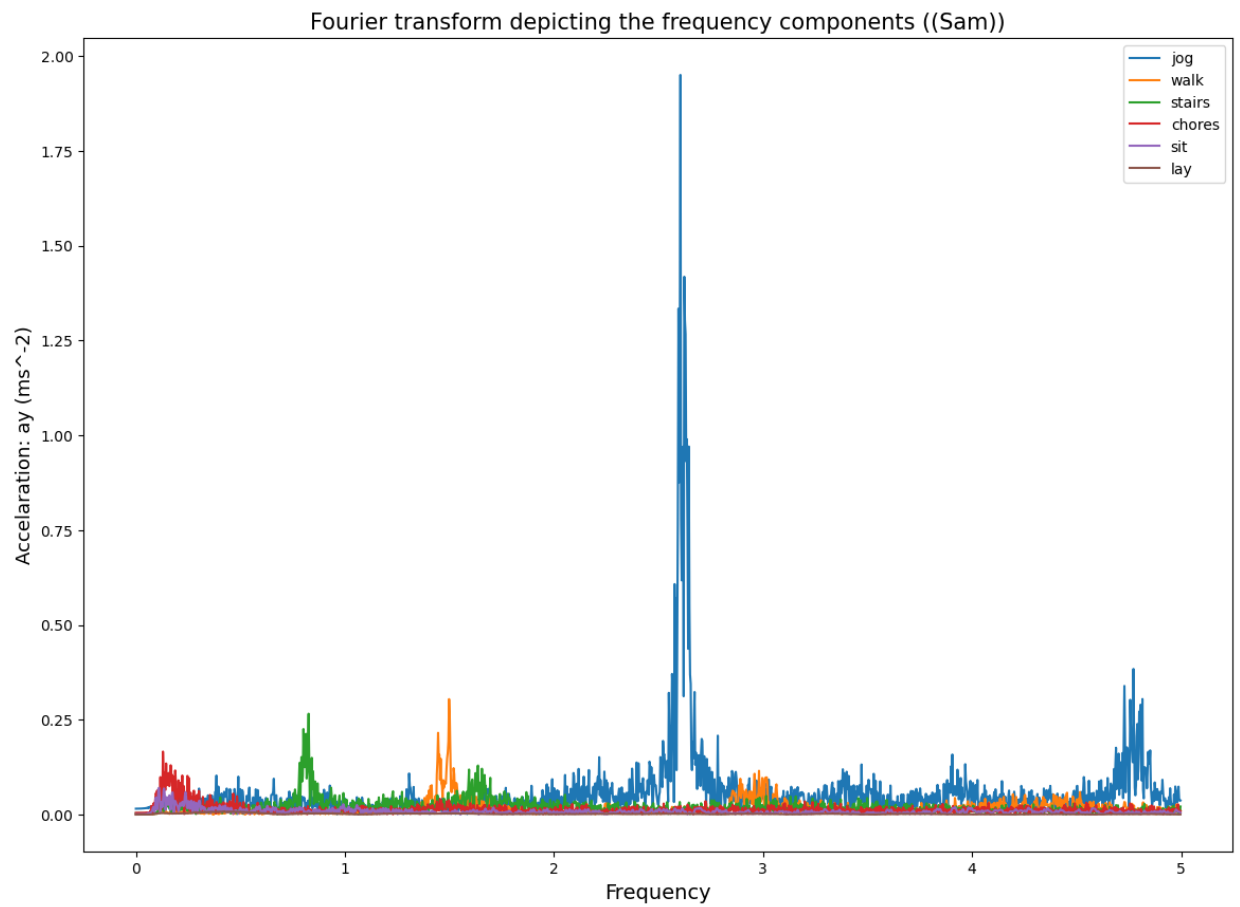


Fig 21: Fourier Transform of Accelerometer Data in ay direction

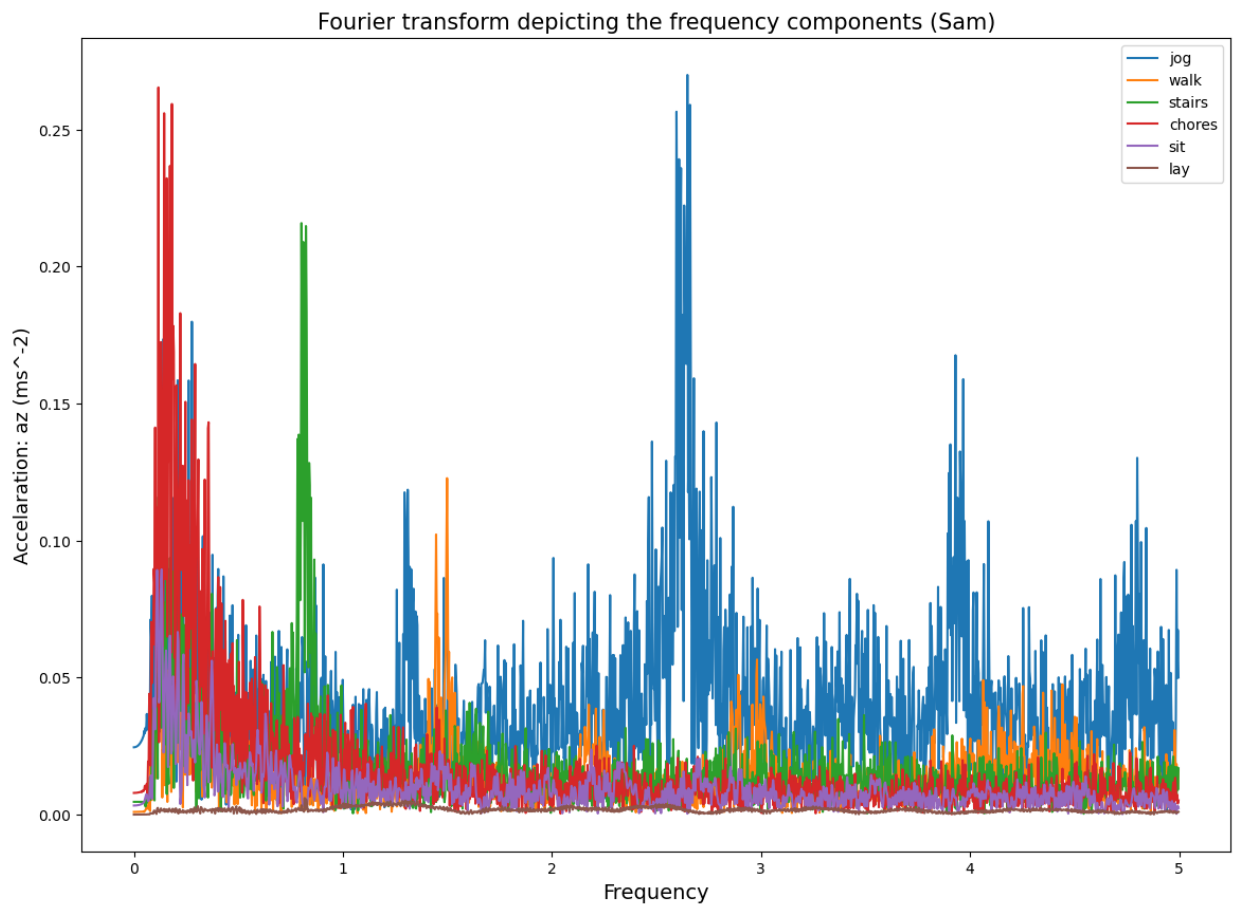


Fig 22: Fourier Transform of Accelerometer Data in az direction

Fig. 20 to 22 show how the amplitude (acceleration) and frequency of Sam's motions are visualized in the Fourier space for the various activities. The trends of such power spectra is well explained due to the nature of each activity. For example - while laying Sam tried his best not too move at all and we the corresponding reflection in the Fourier space.



4.5 Data Set 4: Ordered Activity Data From Mohammad

Similar to Sam, Mohammad took data in the following order as well for 5 minutes.

- jogging
- walking
- stairmaster
- chores
- sitting
- lay

Out[54]:

	time	ax	ay	az	activity
0	0.0	0.260818	4.974080	8.263613	jog
1	0.1	0.346361	4.935197	8.485847	jog
2	0.2	0.514457	4.943572	8.536993	jog
3	0.3	0.436690	4.946563	8.207681	jog
4	0.4	0.462413	4.938188	8.322835	jog
...
17998	1799.8	-0.279960	-1.242473	-9.757931	lay
17999	1799.9	-0.279063	-1.111167	-9.733106	lay
18000	1800.0	-0.175872	-1.107578	-9.752547	lay
18001	1800.1	-0.302991	-1.103091	-9.825528	lay
18002	1800.2	-0.249452	-1.100998	-9.821341	lay

18003 rows × 5 columns

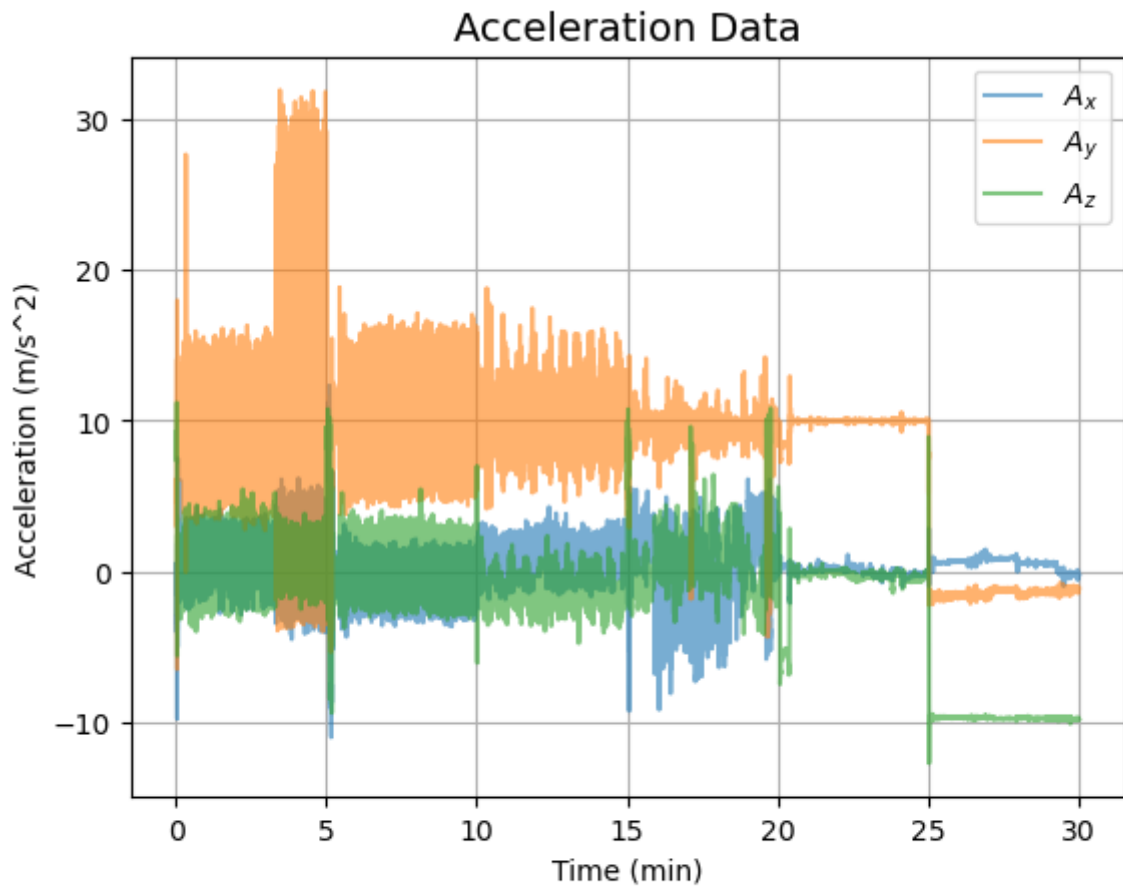


Fig 23: Acceleration Data in x, y, z direction from Mohammad

Fig. 23 is the raw accelerometer data from Mohammad's phone. Like Sam the data is very much representative of the different activities that Mohammad undertook. Since we know, we need to filter out signals from g to see meaningful data in Fourier Space. Now, we filter the data to obtain a dataset that is representative of Mohammad's motions.

Out[58]:

	time	ax	ay	az	activity
0	0.0	0.634097	-0.003368	0.763752	jog
1	0.1	0.746240	-0.110357	1.095651	jog
2	0.2	0.939959	-0.172292	1.261137	jog
3	0.3	0.886725	-0.241779	1.050757	jog
4	0.4	0.935781	-0.324760	1.289341	jog
...
17998	1799.8	-0.078695	-0.045613	-0.002363	lay
17999	1799.9	-0.077723	0.085723	0.022468	lay
18000	1800.0	0.025530	0.089336	0.003033	lay
18001	1800.1	-0.101538	0.093842	-0.069943	lay
18002	1800.2	-0.047957	0.095951	-0.065752	lay

18003 rows × 5 columns

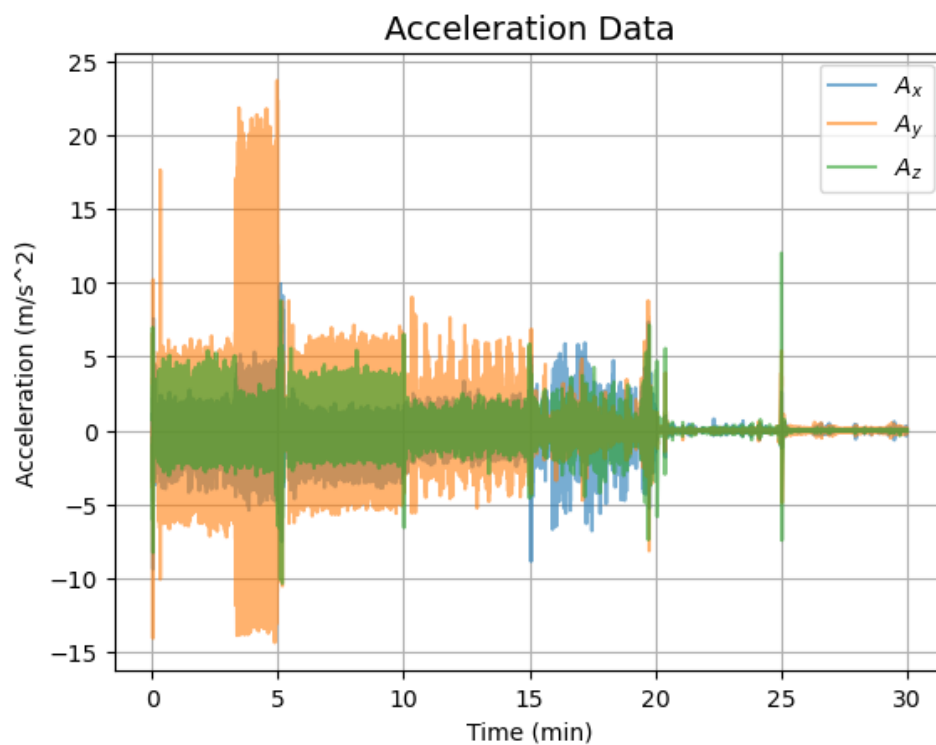


Fig 25: Acceleration Data in x, y, z direction from Mohammad (No Gravity)

Fig. 25 is the accelerometer with the influence of gravity filtered away. Note that this fixed the issue of orientation of the last 5 mins in the data run since Mohammad had the phone oriented differently while laying and the only prominent acceleration affecting the sensor was the influence of gravity.

Fourier transform depicting the frequency components (Mohammad)

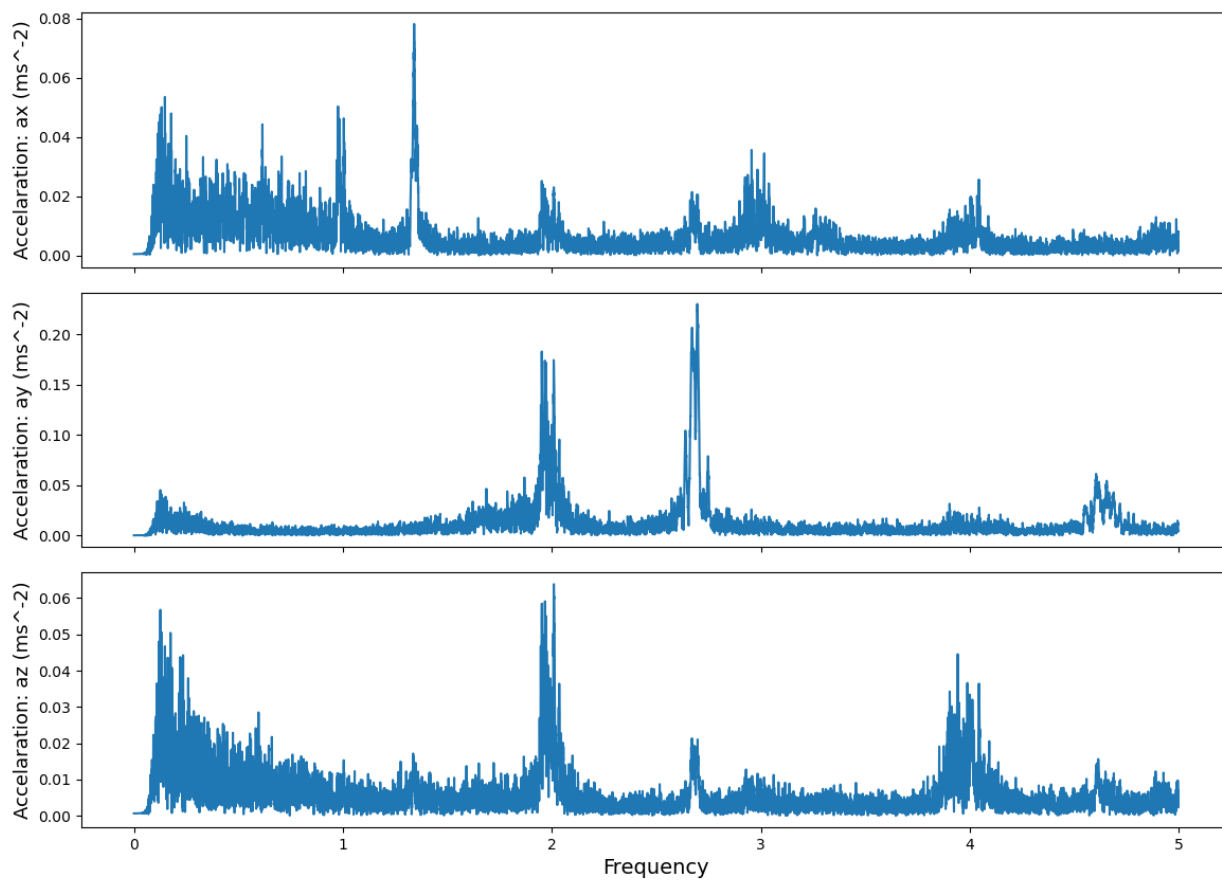


Fig 26: Fourier Transform of Accelerometer Data in x, y, z direction

Fig. 26 also clearly shows that there are prominent trends in the power spectrum. To understand what activity is responsible for what we need to isolate them and color code them.

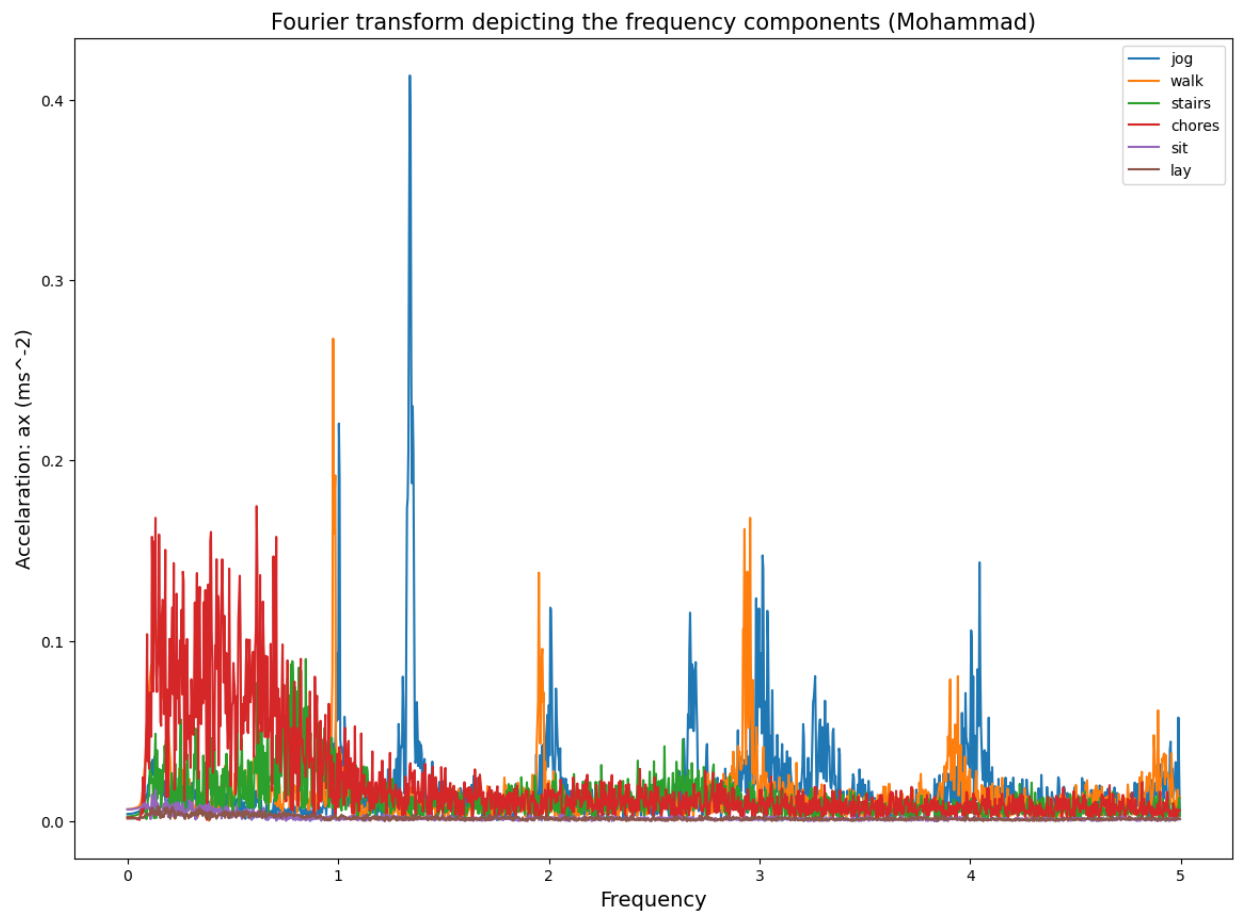


Fig 27: Fourier Transform of Accelerometer Data in ax direction

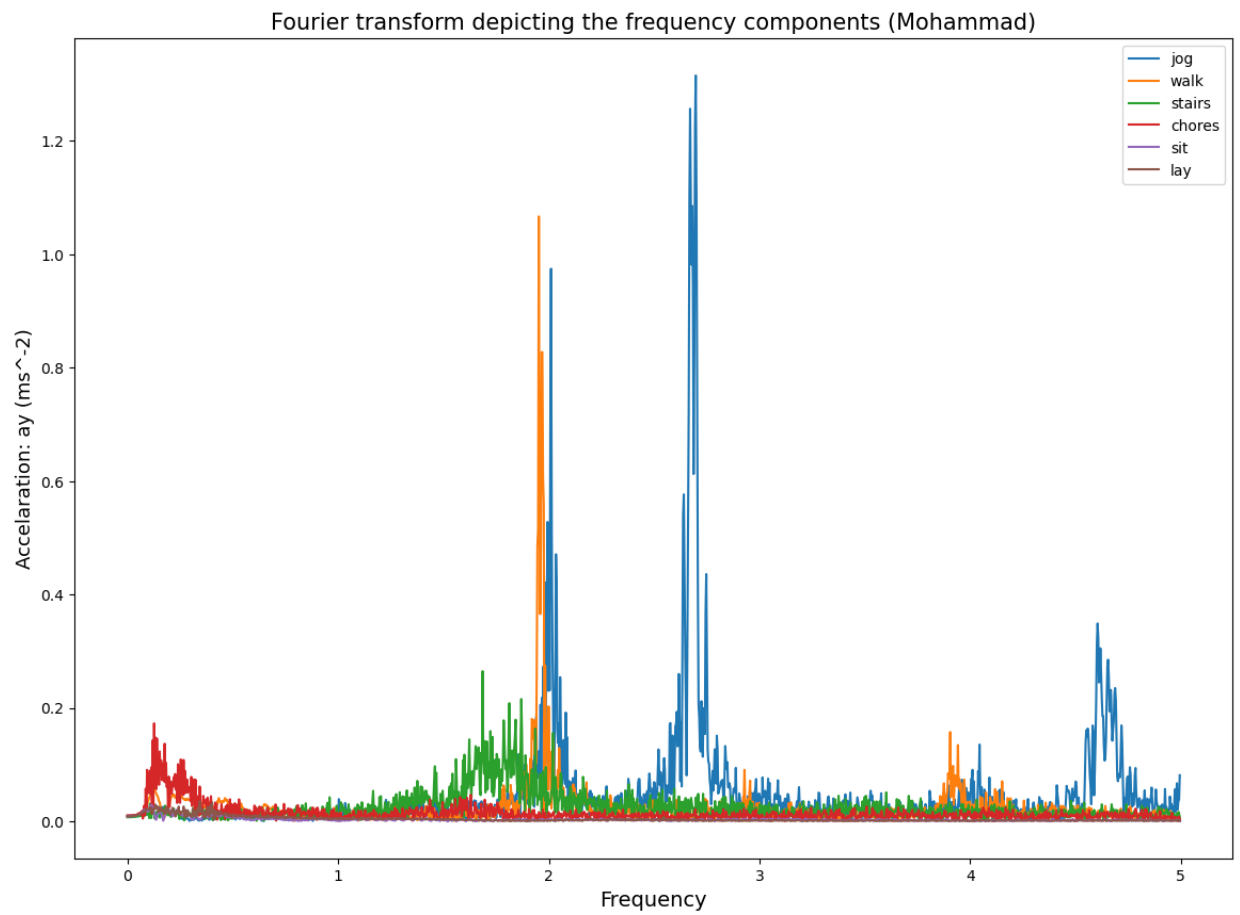


Fig 28: Fourier Transform of Accelerometer Data in ay direction

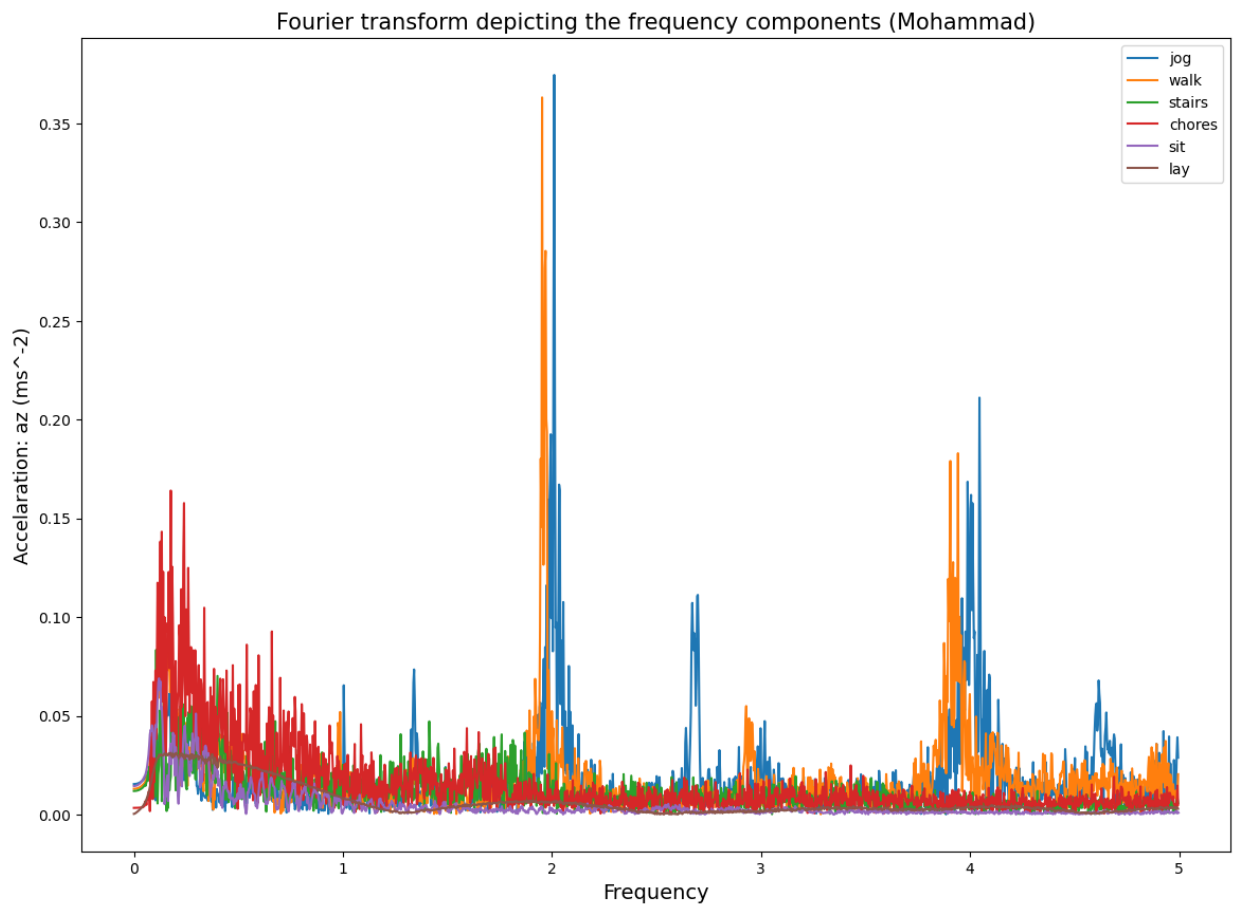


Fig 29: Fourier Transform of Accelerometer Data in az direction

Fig. 27 to 29 show how the amplitude (acceleration) and frequency of Mohammad's motions are visualized in the Fourier space for the various activities. The trends of such power spectra is well explained due to the nature of each activity. For example - while jogging Mohammad changed the speed on the treadmill as he was getting tired and also was irregular with his pace which explains the multi-modal power spectra.

4.6 Comparing Sam's and Mohammad's Data

Now that we know that it is possible to extract activity data from the Fourier Transforms of timeseries accelerometer data, we want to study whether there are any fundamental/universal frequencies of motion associated with a given activity.

4.6.1 Acceleration in X direction

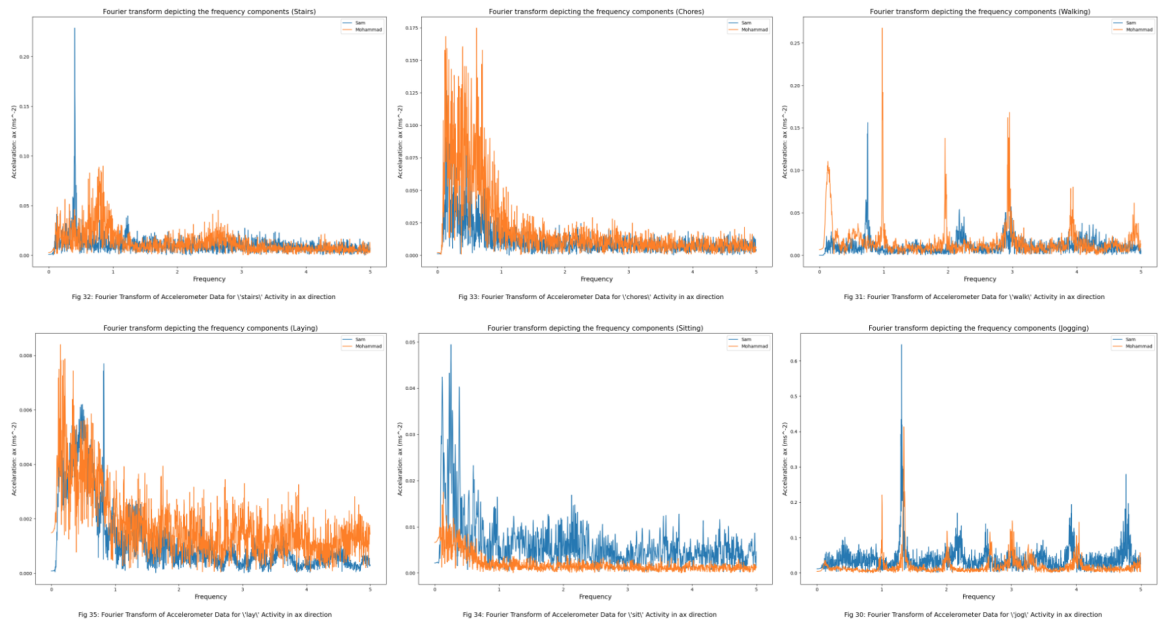


Fig. 30 to 35 compares how Mohammad's and Sam's power spectra for each activity. On first glance, it can be concluded that for certain activities the distribution and for others they don't. This observation is in accordance with the common sense deduction that two bodies laying/sitting have similar kinematics (fidgeting/rolling around aside of course) while two people jogging/walking up the stairs may have different kinematics.

Let's observe the behavior in other dimensions before making any claims regarding the universality of dynamic frequencies for a given activity.

4.6.2 Acceleration in Y direction

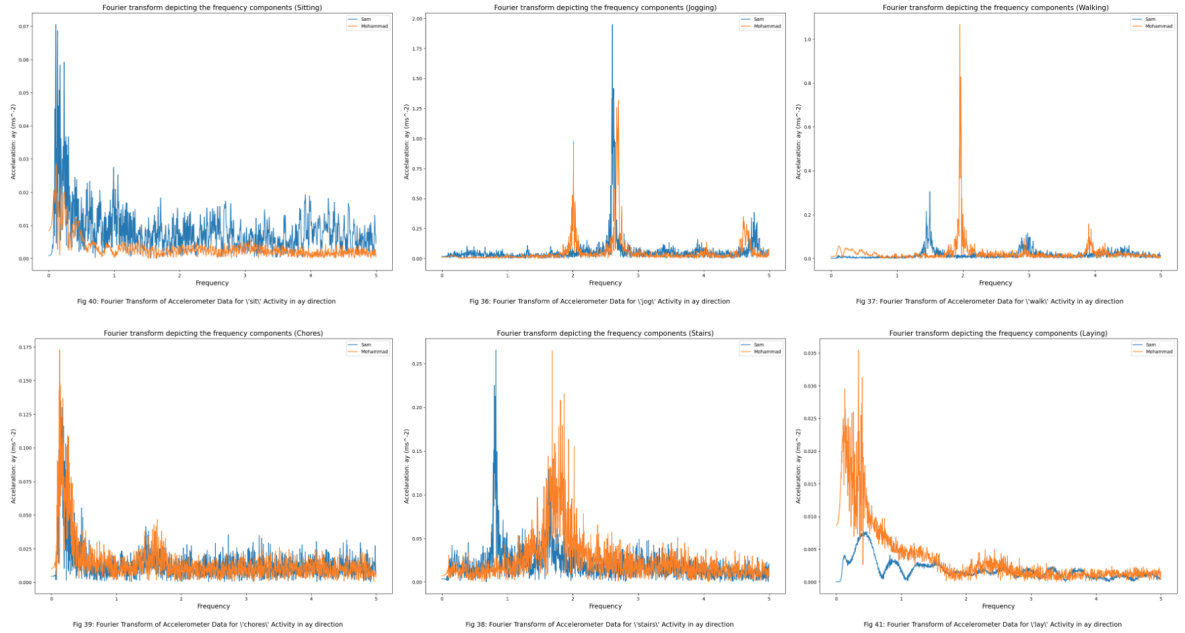


Fig. 36 to 41 also compares how Mohammad's and Sam's power spectra for each activity for the direction parallel the g here of course. Other than the chores data, no other activity reflect similar power spectra distribution. That being said there is no reason to conclude that the frequency of dynamic motion for doing chores is universal since they were not doing the same type of chores and due to the large definition of chores in itself. All the differences, however, are explained according to both Sam's and Mohammad's transcripts as they were doing the activity.

4.6.3 Acceleration in Z direction

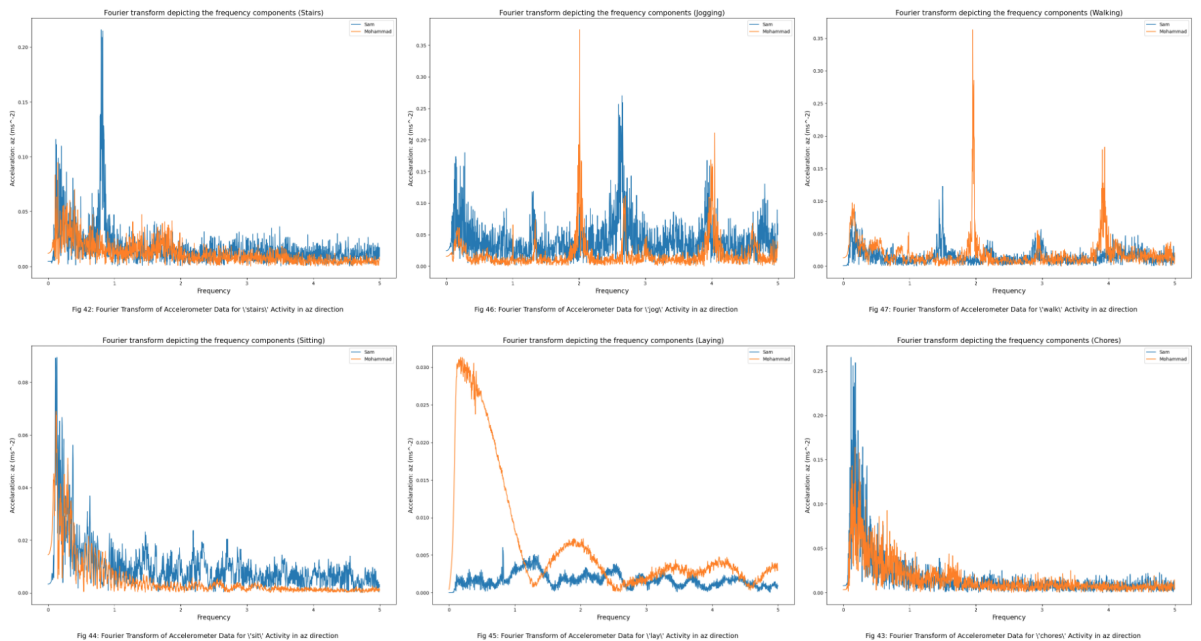


Fig. 42 to 47 also compares how Mohammad's and Sam's power spectra for each activity for the direction perpendicular to the chest pointing outwards of course. These characteristics are in line with the observations made in the previous two subsections.

5 Conclusion & Summary

5.1 Experiment 1

In experiment 1 (See Section 3), we recorded acceleration time series data and implemented a low pass filter with the goal of extracting the value of the gravitational field strength, g . We had three data sets for this experiment - Mohammad driving, Mohammad's flight and Mohammad doing everyday work.

From the first two data sets - Mohammad driving, Mohammad's flight - after implementing the Butter low pass filter, we get the value of g to be 0.19 ± 0.1 and $0.1 \pm 0.1 \text{ ms}^{-2}$ respectively. As evident, the error in both these runs are enormous. We isolated the source of the problem to be the app that Mohammad used. The app automatically filtered out the influence of g which is why we were not able to get access to the data that we need. So after Mohammad changed the app, he recorded a run (10 hours) he was working on his homework, studying, sleeping, walking and using his phone. Based on this run, we get the value of g to be $9.71 \pm 0.1 \text{ ms}^{-2}$. Of course, the value we calculated is accurate with an error of 1% with the accepted value of 9.81 (note 9.81 is within the uncertainty of our value). We further calibrated this dataset by only keeping events where Mohammad's phone had a fixed orientation. With this trimmed and optimized data, we calculated g to be $9.79 \pm 0.1 \text{ ms}^{-2}$ which has an error of 0.16% with the accepted value for g .

This experiment showed that it is possible to extract the value for g accurately from noisy tri-axial accelerometer datasets by using a Butter low-pass filter of order 4 and a phone sensor recording data at 10Hz fidelity.

5.2 Experiment 2

In experiment 2 (See Section 4), we recorded acceleration time series data and implement methods to obtain power spectra of such datasets in the Fourier space. The data takers held the phone upright at the center of their chest with phone screen facing towards body.

The goal of this experiment was to understand whether we can identify distinct activity signatures from acceleration data in Fourier Space and to investigate whether the activity dependent frequencies are universal or not.

For this experiment, we used four data sets in total. The first two data sets were poor due to poor experimental design on our part since the choice of activities and their decisions were not made a-priori. This lead to the two data sets - one from Sam and one from Mohammad - to be of different sizes (1 hour and 5 minutes respectively) and had different activities under consideration. We did get promising results in the power spectra, however, due to the ambiguity and inconsistencies of the experimental conditions, the inferences could not be made on good faith. The snow week had a lot to do with this issue since we did not have reliable communication channels with each other.

After we were aware of the vagueness of our data. We recorded two more data sets where Mohammad and Sam both take data doing the following activities (in order) in 5 minute blocks.

- jogging
- walking
- stairs
- doing chores

- sitting
- laying

For these datasets, we generate two sets of power spectra plots - *one* showing how each activity in a given acceleration axis looks and *the other* comparing Sam's and Mohammad's data for each activity in a given acceleration axis.

From the plots (Fig. 20 - 22 and Fig. 27 - 29), it is evident that it is possible to identify different activities. This answers the first of our research questions. In order to have a dictionary of sorts that translates signals in Fourier space to human activities more controlled and systematic experiments need to be conducted by people that are more representative of the human population itself.

The second question regarding the universality of dynamic motion frequencies for a given activity cannot be answered satisfactorily based on our experiments and data. The design of the experiment in itself introduces natural error in this process which makes fair comparisons not truly possible (e.g. for 5 mins jogging data there were times that Mohammad stopped for a bit due to breathing issues and for the laying part he was moving around compared to Sam who tried his best to lay still). Moreover, since Sam took his data in one contiguous time block there were transitional activities introduced and not all of his activity lasted exactly 5 mins leading to some time based activity tags not being accurate. To answer this question, we still need to devise more controlled and systematic experiments that need to be conducted by people that are more representative of the human population itself.

6 References

- [1] D'Elia, MG & Giudice, Antonio & Graditi, G. & Paciello, Vincenzo. (2013). *Measurement uncertainty on smart phone*. 10.1109/CIVEMSA.2013.6617411. , https://www.researchgate.net/publication/257604942_Measurement_uncertainty_on_smart_phone (https://www.researchgate.net/publication/257604942_Measurement_uncertainty_on_smart_phone)
- [2] Bayat, Akram & Pomplun, Marc & Tran, Duc. (2014). *A Study on Human Activity Recognition Using Accelerometer Data from Smartphones*. Procedia Computer Science. 34. 450-457. 10.1016/j.procs.2014.07.009 , https://www.researchgate.net/publication/262426382_Estimating_heart_rate_variation_during_walkin (https://www.researchgate.net/publication/262426382_Estimating_heart_rate_variation_during_walkir)